

The Risk and Return of Equity and Credit Index Options*

Hitesh Doshi[†] Jan Ericsson[‡] Mathieu Fournier[§] Sang Byung Seo[¶]

December 7, 2023

Abstract

We develop a structural credit risk model, which allows us to price equity/credit indices and their options through the asset dynamics of index constituents. We estimate the model via MLE and find that equity and credit index option prices are well explained out-of-sample. Contrary to recent empirical findings, the two option markets are not inconsistently priced through the lens of our model. Returns on both options, while extreme, do not indicate any evidence of mispricing. Our analysis suggests that jointly addressing the pricing of various instruments requires a balance between three sources of systematic risk: asset, variance, and jump risks.

JEL classification: G12, G13

*We thank Patrick Augustin, Gurdip Bakshi, Hank Bessembinder, Christian Dorion, Bjørn Eraker, Zhiguo He, Kris Jacobs, Mete Kilic, Philippe Mueller, Chay Ornathanalai, Nick Pan, Neil Pearson, Ivan Shaliastovich, Aurelio Vasquez, and seminar participants at the Virtual Derivatives Workshop, Bloomberg Conference, ITAM/HEC Montreal Cancun Derivatives Workshop, Risk Management and Financial Innovation Conference Mont Tremblant, Tsinghua Finance Workshop, Arizona State University, Federal Reserve Board, Temple University, Southern Methodist University, University of Oklahoma, McGill University, University of Houston, and University of Wisconsin-Madison. We gratefully acknowledge the financial support from the Canadian Derivatives Institute. An earlier version of this paper was circulated with the title “Asset Variance Risk and Compound Option Prices.”

[†]Bauer College of Business at the University of Houston; hdoshi@bauer.uh.edu

[‡]Desautels Faculty of Management at McGill University; jan.ericsson@mcgill.ca (corresponding author)

[§]UNSW Business School and Canadian Derivatives Institute; m.fournier@unsw.edu.au

[¶]Wisconsin School of Business at the University of Wisconsin-Madison; sang.seo@wisc.edu

1 Introduction

Option pricing theory, after its emergence in the seventies, not only spawned a new field of research on derivatives pricing but also a new approach to valuing corporate securities. Set forth by Merton (1974), structural credit risk models view corporate securities as option contracts on the issuing firm’s assets. Equity can be seen as a long call and debt as a short put. By extension, options written on corporate securities, such as equity options, can be viewed as options on options or *compound* options (Geske, 1979). This simple idea provides us with a general framework to study the prices and returns on corporate securities and their options jointly.

Recently, this compound option pricing framework has received renewed attention in light of new empirical evidence on the pricing consistency between different index option markets. Collin-Dufresne, Junge, and Trolle (2022) find that it is difficult to reconcile the pricing of options on an equity index (SPX) and those on a credit index (CDX), even with a state-of-the-art structural model. They leave us with a new relative pricing puzzle and conclude that equity and credit markets are not fully integrated. This is a striking finding given a significant body of work suggesting a close link between equity options and various credit instruments.¹

Another question on which such a pricing framework can be brought to bear is on the debate about the magnitude of option returns: are high option returns evidence of mispricing? Bondarenko (2014) documents remarkably high returns from writing SPX put options and argues that these indicate mispricing.² Subsequent work by Broadie, Chernov, and Johannes (2009) calls into question the interpretation that options are mispriced on the basis of their high returns and highlights the importance of jump and volatility risk premia. Building on this work, Chambers, Foy, Liebner, and Lu (2014) argue, in the same setting but with a longer sample, that put returns are too low to be explained by standard option pricing models after all. On top of the seemingly conflicting results for SPX options, which have been the primary focus of the literature to date, our knowledge about the prices and returns on other

¹See, among others, Cremers, Driessen, and Maenhout (2008), Carr and Wu (2011), Collin-Dufresne, Goldstein, and Yang (2012), Culp, Nozawa, and Veronesi (2018), and Cao, Goyal, Xiao, and Zhan (2022).

²This paper became public in 2003, although it was eventually published in 2014.

derivatives and their consistency across different markets remains limited. This is especially so for CDX options, relatively new products that have gained popularity and started actively trading since 2012.

In this paper, we revisit the question of mispricing and seek to broaden the discussion. To this end, we develop a structural credit risk model that enables us to consistently price equity, credit, and associated derivative contracts from the ground up. The model allows firms' assets to exhibit systematic stochastic variance and Poisson jumps. We consider a large cross-section of firms by incorporating idiosyncratic shocks and construct equity and credit indices, which are the model counterparts of the SPX and CDX. Not only does our model link the pricing of equity and credit indices via the asset dynamics of their constituents, but it also endogenously relates the two indices with their options. Furthermore, our framework allows us to compute model-implied returns for these securities as well as to decompose them into compensation for three sources of systematic risk: asset growth risk, variance risk, and jump risk.

We then bring the model to the data. In principle, if we wished to keep track of index constituents one by one, the model would have more state variables than firms in the index. To alleviate this computational burden, we follow the literature and approximate the index with a homogeneous pool of ex-ante identical firms. This so-called large homogeneous pool approximation leads to only two state variables governing the prices of the indices and their options: (i) the asset value of the representative firm and (ii) systematic asset variance. We filter out the time series of these two state variables and estimate the model parameters via maximum likelihood.

Our estimation procedure takes the time series of CDX spread term structures and physical SPX volatility as sole inputs. We observe that the model fits these variables well in-sample. Moreover, the signs and magnitudes of the estimated parameters are economically plausible, as are the time series patterns of the filtered state variables. We also confirm that the estimated model implies reasonable physical metrics such as market leverage, asset Sharpe ratios, and cumulative default probabilities, which provides further confidence in our estimation results. In our model, we specify both the physical and risk-neutral firm asset dynamics and estimate

them using both time series and cross-sectional data. As a result, the estimated model is capable of determining not only price levels but also returns and risk premia.

Next, we examine SPX and CDX options as an out-of-sample exercise based on the estimated parameters and filtered state variables. Although our estimation procedure does not rely on any option data, the empirical implied volatilities are explained well out-of-sample. The model successfully captures the levels of implied volatilities in both option markets. In the moneyness dimension, the model generates a negative volatility skew for SPX options and a positive volatility skew for CDX options that are similar to their empirical counterparts. In both cases, the model-implied volatilities closely track the time series fluctuations in the data, resulting in relatively small pricing errors. The correlations between the model and data are high, around 80% or higher across the board. Importantly, we do not find any significant evidence of absolute or relative mispricing across the two option markets.

We reach a similar conclusion for option returns. Through the lens of our model, realized option returns, while very large, do not appear to suggest any mispricing. We cannot statistically distinguish the data estimates from the model predictions for any option class. The contribution we make is twofold. First, our analysis with SPX options supports and corroborates an earlier conclusion of no mispricing from Broadie, Chernov, and Johannes (2009), using a richer model featuring priced variance and jump risks. Second, we confirm the same finding for CDX options, whose realized and predicted returns are even higher in absolute terms. We note that in this market, prior evidence on prices is scarce and that on returns virtually non-existent.

In sum, the pricing of the SPX and CDX indices as well as their options can jointly be reconciled within our structural option pricing framework. How does our model achieve this? To answer this, we study how exposures to the three sources of systematic risk vary across different instruments. These exposures are important not only for the price dynamics but also for the decomposition of risk premia. While the asset risk premium has the same sign as the exposure to asset growth risk, variance and jump risk premia have opposite signs to their respective exposures because both risks are priced negatively.³

³Since investors dislike either risk, an instrument that pays more in bad times with high variance or jump

Consider first exposures to asset growth risk. Both the SPX and CDX indices have a positive exposure to asset growth risk because the values of equity and debt rise with the firm’s asset value. In terms of magnitude, the SPX exhibits a greater exposure than the CDX, as equity, being more junior than debt, is more leveraged and thus more sensitive to asset fluctuations. In the case of options, SPX calls and CDX puts load positively on asset growth risk, whereas SPX puts and CDX calls load negatively. This is intuitive. Since a negative shock to the equity market (low equity return) is likely to coincide with a positive shock to credit spreads, SPX puts (calls) and CDX calls (puts) pay off in similar states of the world. The signs of exposures to jump risk are the exact opposites to those to asset growth risk because jumps are on average negative in our model, reducing the firm’s assets.

What is more noteworthy are the exposures to variance risk. Perhaps surprisingly, we find that the exposure of the CDX to variance risk is significantly more negative than that of the SPX. This is a result of the interplay between two channels. (i) A rise in asset variance leads to higher discount rates, pushing down the values of both equity and debt. (ii) At the same time, a rise in asset variance raises the values of options written on the firm’s assets, regardless of whether they are calls or puts, through a “vega effect.” Thus, equity (long call) increases and debt (short put) decreases in value. In the case of debt, the two channels lead in the same direction, making the exposure heavily negative. In the case of the SPX, the two channels work in opposite directions, offsetting each other. This may explain the seemingly puzzling empirical finding that selling CDX straddles provides much higher returns than selling SPX straddles (Collin-Dufresne, Junge, and Trolle, 2022); the CDX is more sensitive to variance risk than the SPX. This property is inherited by CDX options, resulting in interesting patterns in their exposures to variance risk.

Next, we revisit the relative pricing puzzle posed by Collin-Dufresne, Junge, and Trolle (2022). In essence, they find that their model generates too low implied volatilities for CDX options when it is fitted to match the CDX spread and implied volatilities for SPX options. Similar to their calibration, we take our estimated model and search for the values of the two risk (i.e., a positive exposure) serves as a hedge; investors are willing to take a negative risk premium for such an instrument.

state variables that match the median CDX spread and at-the-money SPX implied volatility. We find that our model generates a CDX implied volatility that is close to and slightly larger than its data counterpart.

Why do we obtain such different results? While our model and theirs differ in the precise assumptions about capital structure and default, both models assume identical asset dynamics with stochastic variance and jump risks. Hence, we are able to map the parameters of Collin-Dufresne, Junge, and Trolle (2022) into ours. When we repeat the fitting exercise under their parametrization, we do recover the underpricing issue, which suggests that differences in parametrization play a role.

Overall, our analysis suggests that jointly addressing the pricing of CDX, SPX options, and CDX options requires finding the right balance between different sources of risk. There are two tensions at play. The first is between systematic risk and idiosyncratic risk, whose shares of total risk have important implications for index options but have less to do with the CDX spread. The second tension exists among different sources of systematic risk, as asset growth risk, variance risk, and jump risk disproportionately affect different instruments based on their exposures. In conclusion, the way in which the model is configured with different sources of risk is pivotal for capturing the joint pricing of various market instruments.

Related literature

Our work is related to several strands of literature. The first consists of recent studies that link credit and equity derivative markets. Cremers, Driessen, and Maenhout (2008) use equity and option prices to estimate jump risk premia in order to predict credit spreads. Collin-Dufresne, Goldstein, and Yang (2012) use a model fitted to long-dated SPX options and CDX term structures to value CDX tranches out-of-sample. Culp, Nozawa, and Veronesi (2018) convert option prices into credit spreads by hypothesizing pseudo firms in a model-free setting. What all of these papers have in common is that they price corporate credit instruments out-of-sample using a model estimated from the data on other markets. There are at least two key differences between this prior work and ours. First, our estimation goes in a different direction in the sense that we use the data on credit spreads (CDX term structures) to obtain out-of-

sample predictions for options. Second, we link four markets consistently: the SPX and CDX markets together with their corresponding option markets. Like much of previous studies, we find that the four markets are closely related.

Our paper contributes to the extensive literature on option pricing. The empirical option literature has primarily been based on a reduced-form approach, which exogenously specifies the underlying process and focuses on modeling the joint dynamics of the underlying and derivative prices. Notable examples include, but are not limited to, Bakshi, Cao, and Chen (1997), Pan (2002), Bates (2003), Eraker (2004), and Christoffersen, Jacobs, Ornathanalai, and Wang (2008). Our approach significantly differs from theirs as we rely on a structural framework à la Geske (1979) where both the underlying and derivative prices endogenously derive from the firm's asset dynamics. An advantage of using a structural approach in our paper is that the indices that underlie SPX and CDX options are themselves contingent claims. For example, the CDX is, just like CDX options, a contingent claim on the assets of the constituent firms. Hence, using the time series of CDX spreads in the estimation is informative not just for the physical dynamics but also for the risk-neutral dynamics. This allows us to estimate our model without using any option-based information and study the two option markets out-of-sample. Achieving this is difficult, if not impossible, in a standard reduced-form model where the underlying dynamics are specified exogenously. In this case, realizations of the underlying are only informative about the physical measure, and thus the use of option data is necessary for estimating the risk-neutral dynamics.

Several studies demonstrate that more general non-affine option pricing models provide a better fit to the cross-section of equity option prices. See, for instance, Jones (2006) who develops a non-affine stochastic volatility model to study index option prices, and Eraker and Wang (2015) who develop a nonlinear model of the variance premium. Because equity and credit derivatives are compound options in our model, their dynamics are highly nonlinear and display non-affine features. The main distinction from previous studies is that nonlinearities in the index dynamics within our framework arise endogenously as a function of leverage and unlevered asset dynamics.

Lastly, our work concerns the literature studying the magnitudes and properties of variance, jump, and tail risk premia in financial securities. For seminal contributions to this literature, see, among others, Bates (2000), Coval and Shumway (2001), Pan (2002), Eraker, Johannes, and Polson (2003), Carr and Wu (2009), Todorov (2010), Andersen, Fusari, and Todorov (2020), and Andersen, Todorov, and Ubukata (2021). Most existing studies in this literature focus on equity index and index option markets. Our contribution is to broaden the study of variance and jump risk premia to multiple markets simultaneously and to trace the sources of risk premia in these markets back to those of the underlying assets of the firm.

The rest of the paper proceeds as follows. Section 2 describes our model. Section 3 details the data and estimation approach. Section 4 provides comparative statics to help understand the model mechanism. Importantly, the relative pricing puzzle of Collin-Dufresne, Junge, and Trolle (2022) is replicated and resolved. Section 5 reports on our model's empirical validation in-sample and out-of-sample and provides implications for option returns. Section 6 concludes.

2 Model

In this section, we develop a structural credit risk model which allows us to consistently price equity, credit, and associated derivative contracts from the ground up. We first introduce the asset dynamics for individual firms and the economy's stochastic discount factor (Section 2.1). The pricing of corporate securities follows (Section 2.2). We then construct the equity and credit indices and study the pricing of index options (Section 2.3). Lastly, we show that the expected returns on these indices and options can be decomposed into compensation for the three systematic risk exposures in our model (Section 2.4).

2.1 Asset and variance risk

We consider a cross-section of firms $j \in \{1, \dots, N\}$ whose asset dynamics under the physical measure \mathbb{P} are driven by the systematic asset factor A_t^m as well as two types of idiosyncratic shocks:

$$\frac{dA_t^j}{A_t^j} = \frac{dA_t^m}{A_t^m} + \sigma_j dW_t^j + \nu^j dN_t^j - \lambda^j \nu^j dt, \quad (1)$$

where dW_t^j is a standard Brownian motion and dN_t^j is a Poisson process. We use σ_j to denote the time-invariant volatility parameter for diffusive idiosyncratic risk. The idiosyncratic jump intensity is also, in the interests of parsimony, constant with $\mathbb{E}_t[dN_t^j] = \lambda^j dt$, where $\mathbb{E}_t[\cdot]$ denotes a time- t conditional physical expectation. The relative change in asset value caused by the occurrence of an idiosyncratic jump is deterministic with a value of $\nu^j = (e^{z^j} - 1)$.

As in Du, Elkamhi, and Ericsson (2019), the dynamics of the systematic asset factor A_t^m and its stochastic variance V_t are characterized by the following equations under \mathbb{P} :

$$\frac{dA_t^m}{A_t^m} = (\mu_t - q) dt + \sqrt{V_t} dW_t^A + \nu_t^m dN_t^m - \lambda_t^m \bar{\nu}^m dt, \quad (2)$$

$$dV_t = \kappa(\theta - V_t)dt + \delta\sqrt{V_t}dW_t^V, \quad (3)$$

where μ_t is the expected return on the unlevered “market” and q is the corresponding payout

rate. The systematic diffusive variance V_t follows a square-root process where κ , θ , and δ represent the mean-reversion speed, long-run mean, and volatility of variance, respectively. To model the correlation between systematic asset return and variance shocks, we assume that $dW_t^A = \rho dW_t^V + \sqrt{1 - \rho^2} dW_t^{A\perp V}$ where dW_t^V and $dW_t^{A\perp V}$ are two mutually independent Brownian motions. When $\rho < 0$, systematic asset variance is high when systematic asset return is low. This case implies a negative skewness in the distribution of unlevered market returns, consistent with empirical evidence.⁴

In addition to systematic diffusive risk, we allow for systematic jumps captured by the jump process $\nu_t^m dN_t^m$, where dN_t^m is another Poisson process counting the occurrence of systematic jumps. Its intensity, $\mathbb{E}_t[dN_t^m] \equiv \lambda_t^m dt$, is time-varying and assumed to be proportional to V_t such that $\lambda_t^m = \eta_m V_t$. As a result, systematic jumps are more likely to occur during market downturns when systematic variance is relatively high. Conditional on a systematic jump, the relative change in asset value is a random variable defined as $\nu_t^m \equiv (e^{Z_t^m} - 1)$. We assume that Z_t^j is normally distributed with time-invariant parameters $Z_t^m \sim N(z_m, \gamma_m^2)$. Accordingly, the expected systematic jump size is calculated as $\bar{\nu}^m = \mathbb{E}_{Z^m}[e^{Z_t^m} - 1]$, where $\mathbb{E}_{Z^m}[\cdot]$ represents an expectation taken with respect to the time-invariant distribution of Z_t^m .

In the absence of arbitrage, there exists a stochastic discount factor (SDF), which allows us to price firms' financial claims. Following the literature on variance and jump risks, we assume that the SDF is exponentially affine in aggregate risks:

$$\frac{d\phi_t}{\phi_t} = -r_f dt - \xi_{A\perp V} \sqrt{V_t} dW_t^{A\perp V} - \xi_V \sqrt{V_t} dW_t^V + (e^{\xi_m Z_t^m} - 1) dN_t^m - \lambda_t^m \bar{\nu}^{\xi_m} dt, \quad (4)$$

where r_f is the risk-free rate and $\xi_{A\perp V}$, ξ_V , and ξ_m represent the market prices of diffusive asset growth, variance, and jump risks, respectively. The expected jump size of the SDF is denoted by $\bar{\nu}^{\xi_m} = \mathbb{E}_{Z^m}[e^{\xi_m Z_t^m} - 1]$. Note that firms' idiosyncratic risks are deliberately not priced in the model.

According to Girsanov's theorem, this SDF implies the following dynamics of A_t^m and V_t

⁴For discussions on the presence of negative skewness in the distribution of systematic risks, see Berger, Dew-Becker, and Giglio (2020), among others.

under the risk-neutral measure \mathbb{Q} :

$$\frac{dA_t^m}{A_t^m} = (r_f - q) dt + \sqrt{V_t} dW_t^{A,\mathbb{Q}} + \nu_t^{m,\mathbb{Q}} dN_t^{m,\mathbb{Q}} - \lambda_t^{m,\mathbb{Q}} \bar{\nu}^{m,\mathbb{Q}} dt, \quad (5)$$

$$dV_t = \kappa^{\mathbb{Q}}(\theta^{\mathbb{Q}} - V_t) dt + \sigma \sqrt{V_t} dW_t^{V,\mathbb{Q}}, \quad (6)$$

where $dW_t^{A,\mathbb{Q}} = \rho dW_t^{V,\mathbb{Q}} + \sqrt{1 - \rho^2} dW_t^{A \perp V,\mathbb{Q}}$, $\kappa^{\mathbb{Q}} = \kappa + \delta \xi_V$, and $\theta^{\mathbb{Q}} = \kappa \theta / \kappa^{\mathbb{Q}}$.⁵ When systematic jump risk is priced, it simultaneously shifts the intensity and the mean of systematic jumps under \mathbb{Q} . Specifically, the risk-neutral jump intensity becomes $\mathbb{E}_t^{\mathbb{Q}}[dN_t^{m,\mathbb{Q}}] = \lambda_t^{m,\mathbb{Q}} dt = \lambda_t^m e^{\xi_m z^m + \frac{1}{2}(\xi_m)^2 \gamma_m^2} dt$ and the random jump size is $\nu_t^{m,\mathbb{Q}} = (e^{Z_t^{m,\mathbb{Q}}} - 1)$ with $Z_t^{m,\mathbb{Q}} \sim N(z_m^{\mathbb{Q}}, \gamma_m^2)$ for which $z_m^{\mathbb{Q}} = z_m + \xi_m \gamma_m^2$. Given that idiosyncratic risk is not priced, the risk-neutral dynamics of A_t^j are obtained by inserting equations (5) and (6) into equation (1).

Given equations (2) and (5), the unlevered asset risk premium, or the difference between the \mathbb{P} - and \mathbb{Q} -expected asset return, is given by:

$$(\mu_t - r_f) dt = \left(\sqrt{1 - \rho^2} \xi_{A \perp V} + \rho \xi_V \right) V_t dt + \lambda_t^m \mathbb{E}_{Z^m} \left[(1 - e^{Z_t^m}) (e^{\xi_m Z_t^m} - 1) \right] dt. \quad (7)$$

The first term captures the compensation for diffusive asset growth and variance risks while the second corresponds to the systematic asset jump risk premium.

2.2 Pricing of corporate securities

Following Leland (1994), we assume that each firm issues a consol bond. Firm j declares bankruptcy when the firm's asset value falls to a certain threshold. In the model, the timing of the firm's default τ_j corresponds to the first time at which the asset value A_t^j in equation (1) hits the default barrier A_D : $\tau_j = \inf\{s \geq t | A_s^j \leq A_D\}$.

Prices of a firm's securities and contingent claims depend on the risk-neutral distribution of τ_j and are a function of two key quantities: (i) the present value of a dollar received at default $P_D(A_t^j, V_t) = \mathbb{E}_t^{\mathbb{Q}}[e^{-r_f(\tau_j - t)}]$ and (ii) the cumulative risk-neutral default probability $G(A_t^j, V_t, T) = \mathbb{E}_t^{\mathbb{Q}}[\mathbf{1}_{\tau_j \leq T}]$ over the next T years. Equipped with these, we are able to price any

⁵Applying Girsanov's theorem, we have $dW_t^{A \perp V} = dW_t^{A \perp V,\mathbb{Q}} - \xi_{A \perp V} \sqrt{V_t} dt$ and $dW_t^V = dW_t^{V,\mathbb{Q}} - \xi_V \sqrt{V_t} dt$.

security issued by the firm as well as associated derivative contracts. The Internet Appendix contains details about the estimation of $P_D(A_t^j, V_t)$ and $G(A_t^j, V_t, T)$ for a given set of structural parameters in our setup.⁶

To begin, we calculate the firm's debt value $D(A_t^j, V_t)$ as the present value of future coupon payments plus the recovery value of the firm upon default:

$$D(A_t^j, V_t) = \frac{c}{r_f} [1 - P_D(A_t^j, V_t)] + (1 - \alpha)A_D P_D(A_t^j, V_t), \quad (8)$$

where c is the coupon and α is the liquidation cost. For simplicity, we assume that firms have the same coupon, liquidation cost, default barrier, and idiosyncratic diffusive and jump risk parameters. With leverage, a firm's value deviates from its unlevered counterpart A_t^j for two reasons. First, the firm enjoys tax benefits arising from its debt. If the tax rate is ζ , the present value of future tax shields is $\frac{\zeta c}{r_f} [1 - P_D(A_t^j, V_t)]$. However, this benefit comes with a cost. The debt exposes the firm to the risk of default, and the present value of future bankruptcy costs is $\alpha A_D P_D(A_t^j, V_t)$. Hence, the levered firm value can be expressed as:

$$L(A_t^j, V_t) = A_t^j + \frac{\zeta c}{r_f} [1 - P_D(A_t^j, V_t)] - \alpha A_D P_D(A_t^j, V_t).$$

Since the firm's equity is a residual claim, its value is calculated as the difference between the levered firm value and the debt value, $L(A_t^j, V_t) - D(A_t^j, V_t)$. It is given by:

$$E(A_t^j, V_t) = A_t^j - \frac{(1 - \zeta)c}{r_f} [1 - P_D(A_t^j, V_t)] - A_D P_D(A_t^j, V_t). \quad (9)$$

We also consider the pricing of a CDS contract, which involves two parties: the protection buyer and the protection seller. The protection buyer makes quarterly premium payments to the protection seller until the maturity of the contract (T) or until the firm's default, whichever comes first. Upon default, the protection seller must buy the defaulted bond at par from the

⁶More precisely, our estimation strategy builds on Du, Elkamhi, and Ericsson (2019) who develop a simulation approach to obtain the smooth mapping from a given pair of state variables (A_t^j, V_t) to $P_D(\cdot)$ and $G(\cdot, T)$ using two-dimensional Chebyshev polynomials.

protection buyer, thus absorbing the default loss.⁷

For every basis point (bp) spread per annum, the present value of future premium payments (or premium leg) is known as the risky PV01, or RPV01. In exchange for making premium payments, the protection buyer acquires a promise to make him whole in the event of losses arising in default. We denote the present value of a contingent protection payment (or protection leg), ProtLeg. By definition, the CDS spread is the fair market spread that equates the premium leg with the protection leg. It satisfies

$$S(A_t^j, V_t, T) = \frac{\text{ProtLeg}(A_t^j, V_t, T)}{\text{RPV01}(A_t^j, V_t, T)}. \quad (10)$$

We refer the reader to Appendix A for details about the computation of the premium leg, protection leg, and fair market CDS spread.

2.3 Equity and credit indices and their options

So far, we have defined the dynamics of a firm’s asset value and described the valuation of corporate securities and CDS contracts. Ultimately, our goal is to value equity and credit indices as well as option contracts written on them. To this end, we first define the value of an index and then discuss how it can be mapped to study the S&P 500 index (in short, SPX) or the CDX North American Investment Grade Index (in short, CDX).⁸ We then elaborate on the pricing of SPX and CDX options.

Consider an equally weighted index I_t with N constituents, which is defined as

$$I_t \equiv I(A_t^1, \dots, A_t^N, V_t) = \frac{1}{N} \sum_{j=1}^N f(A_t^j, V_t), \quad (11)$$

where f is defined by equation (9) for the SPX and by equation (10) for the CDX. In our implementation, we consider a cross-section of 500 firms ($N = 500$), constituting each index.⁹

⁷In practice, this settlement is often done instead as a cash payment based on a post-default market value determined by a third party.

⁸The CDX tracks an equally-weighted basket of investment-grade single-name CDS contracts.

⁹We make an implicit assumption that the equity index and the credit index are both based on the same pool of underlying firms. In practice, the SPX consists of 500 firms while the CDX is composed of 125 firms.

Without any further assumptions, modeling the dynamics of an index composed of 500 firms would require keeping track of 501 state variables over time (i.e., A_t^j for $j = 1, \dots, 500$ and V_t).

To alleviate this computational challenge, we follow the literature and approximate the index with a homogeneous pool of ex-ante identical firms (see, e.g., Vasicek, 2002; Collin-Dufresne, Goldstein, and Yang, 2012; Seo and Wachter, 2018; Collin-Dufresne, Junge, and Trolle, 2022). We hypothesize a firm that represents the average of the firms in the index and denote it by superscript r , instead of j . Like other firms, its asset dynamics are described by equation (1). At each pricing date t , the homogeneity assumption, $A_t^j = A_t^r$ for all $j \in \{1, \dots, N\}$, implies that the index satisfies $I_t = \frac{1}{N} \sum_{j=1}^N f(A_t^r, V_t) = f(A_t^r, V_t)$. This leaves us with only two state variables to keep track of: the representative asset value, A_t^r , and the common factor variance, V_t . It is important to note the distinction between levels and dynamics. The representative asset value dynamics are obtained from equation (1) with $j = r$ and are impacted by idiosyncratic shocks. However, the dynamics of the index will see idiosyncratic shocks diversified away. See the Internet Appendix for further details about index dynamics.

In our empirical analysis below, we use call and put option contracts on the SPX and the CDX. The values of calls and puts written on one of these indices can be calculated as:

$$c(A_t^r, V_t, K, T) = e^{-rfT} \mathbb{E}_t^{\mathbb{Q}} [\max(I_{t+T} - K, 0)], \quad (12)$$

$$p(A_t^r, V_t, K, T) = e^{-rfT} \mathbb{E}_t^{\mathbb{Q}} [\max(K - I_{t+T}, 0)], \quad (13)$$

where I_t represents either the SPX or the CDX. To calculate option prices at time t , we simulate forward 5,000 paths of 500 ex-ante homogeneous firms and systematic variance under the risk-neutral measure. While all of the firms are given the same initial value ($A_t^j = A_t^r$ for $j = 1, \dots, 500$), their simulated asset values in the future can deviate from one another due to distinct idiosyncratic shocks (W^j and N^j). For each path, we obtain 500 simulated asset values A_{t+T}^j together with the simulated systematic variance V_{t+T} from which a given index

However, Collin-Dufresne, Junge, and Trolle (2022) show by comparing various key characteristics, such as ratings, leverage, and total/idiosyncratic asset volatility, that modeling the two indices assuming the same number of constituents is relatively innocuous in a setting such as ours.

value is determined using equation (11). We then calculate the conditional expectations in equations (12) and (13) as the averages across the simulated paths.

2.4 Expected returns and risk premia

Our valuation framework enables us to derive how exposures to asset, variance, and jump risks determine expected returns on corporate securities and options. As we argue next, jointly analyzing credit and equity index options will prove to be informative about how the three sources of systematic risk drive derivatives returns across the two markets.

To lay out the main prediction of our model, consider an arbitrary instrument $g_t \equiv g(A_t^r, V_t)$. This could be a tradeable unit of an index ($g = I$) or an option contract written on such an index ($g = c$ or p). By Ito's lemma, we can show that

$$\mathbb{E}_t \left[\frac{dg_t}{g_t} \right] - E_t^{\mathbb{Q}} \left[\frac{dg_t}{g_t} \right] = \underbrace{\Delta_{A,t} (\mu_t - r_f) dt}_{\text{Asset risk premium}} + \underbrace{\Delta_{V,t} (\delta \xi_V V_t) dt}_{\text{Variance risk premium}} + \underbrace{\lambda_t^m \mathbb{E}_{Z^m} [-\Delta_{N,t} (e^{\xi_m Z_t^m} - 1)] dt}_{\text{Jump risk premium}}, \quad (14)$$

where $\Delta_{A,t} \equiv \frac{\partial g_t / g_t}{\partial A_t^r / A_t^r}$, $\Delta_{V,t} \equiv \frac{\partial g_t / g_t}{\partial V_t}$, and $\Delta_{N,t} \equiv \frac{\partial g_t / g_t}{\partial N_t} = \frac{g(A_t^r e^{Z_t^m}, V_t) - g_t}{g_t}$ are the exposures of the instrument to asset, variance, and jump risks, respectively. Under the risk-neutral measure, the total expected return on any tradeable instrument equals the risk-free rate: $E_t^{\mathbb{Q}} \left[\frac{dg_t}{g_t} \right] + q_g dt = r_f dt$ where q_g is a dividend/income yield from the instrument, if any. Hence, the left-hand side of equation (14) equals $\mathbb{E}_t \left[\frac{dg_t}{g_t} \right] + q_g dt - r_f dt$, which represents the instantaneous expected excess return or risk premium on g . Note that $\Delta_{N,t}$ is a random variable, which depends on the random jump size Z_t^m . The expectation in the last term is thus taken with respect to the time-invariant distribution of Z_t^m . For notational convenience, we denote $\mathbb{E}_{Z^m} [\Delta_{N,t}]$ by $\bar{\Delta}_{N,t}$.

Equation (14) reveals that the expected excess return can be decomposed into three terms, which correspond to the three sources of systematic risk. The first term, which we label as *asset risk premium*, captures the compensation for the instrument's exposure to asset value fluctuations. By definition, $\Delta_{A,t}$ is the elasticity of the instrument price g_t with respect to the asset value A_t^r . When the asset value moves by 1%, the instrument price moves by $\Delta_{A,t}$ %. If

the instrument price increases with the asset value ($\Delta_{A,t} > 0$), the instrument earns a positive asset risk premium $\Delta_{A,t}(\mu_t - r_f)$ given $\mu_t - r_f > 0$.

The second term, which we call *variance risk premium*, arises due to the instrument's exposure to variance risk. Since investors' marginal utility (equivalently, the SDF in equation (4)) rises in bad times with high variance, the market price of variance risk ξ_V is typically negative. Consequently, an instrument that is positively exposed to aggregate variance risk ($\Delta_{V,t} > 0$) bears a negative variance risk premium ($\Delta_{V,t}(\delta\xi_V V_t) < 0$). This is intuitive. An instrument that pays more in high SDF periods (when V_t is high) serves as a hedge. Hence, investors are willing to pay a premium to hold such an instrument, leading to a negative variance risk premium.

The third and last term contributing to the expected excess return is referred to as *jump risk premium*. Like any risk premium, this term originates from the comovement between the instrument price and the SDF. In fact, the two variables simultaneously change when a systematic jump occurs: the relative decrease in the instrument price is $-\Delta_{N,t}$ whereas the relative increase in the SDF is $(e^{\xi_m Z_t^m} - 1)$. Therefore, conditional on the occurrence of a jump, the tendency of the two variables to move together is captured by $\mathbb{E}_{Z^m}[-\Delta_{N,t}(e^{\xi_m Z_t^m} - 1)]$. The jump risk premium in equation (14) is obtained from this expression multiplied by the jump intensity λ_t^m , taking into account the likelihood of a jump. In a typical setup where investors dislike jumps that are on average negative ($\xi_m < 0$), the jump risk premium is positive for an instrument with a negative exposure ($\Delta_{N,t} < 0$). An instrument that performs poorly in high SDF periods (with systematic jump realizations) makes investors more exposed to business cycle fluctuations. Investors are reluctant to hold such an instrument, inducing a positive risk premium.

3 Data and estimation

3.1 Data

The model estimation is based on the daily time series of the following five variables: the CDX spreads with 3-, 5-, 7-, and 10-year maturities and the physical SPX volatility. The data on the CDX are obtained from Markit. The physical volatilities of the SPX are proxied by the conditional volatilities obtained from fitting an NGARCH model (with a skewed student t-distribution) to daily SPX returns.¹⁰ The daily time series of the SPX are from the CRSP dataset. For estimation purposes, our sample period begins in June 2004, from which the CDX data become available, and ends in November 2020.

We also collect pricing data on 1-month SPX options and CDX options. These data serve two purposes: (i) to conduct an out-of-sample analysis of model performance and (ii) to revisit the puzzle documented by Collin-Dufresne, Junge, and Trolle (2022) that the two option markets are inconsistently priced. We download SPX option prices from OptionMetrics. For a given trading day, we convert SPX option prices into Black-Scholes-implied volatilities and construct the volatility surface via polynomial interpolation. Then, we keep implied volatilities at 95, 100, and 105% moneyness values as measured by the ratio of strike price to underlying index value. The sample period for SPX options spans the same period covered by our estimation, beginning in June 2004 and ending in November 2020. The quotes on CDX options are provided by Markit. CDX options are essentially credit swaptions, which provide the holder the right to enter into an index credit default swap (i.e., CDX) either as the protection buyer (payer swaptions or CDX calls) or as the protection seller (receiver swaptions or CDX puts). These options are quoted in terms of Black-implied volatilities, and we select implied volatilities whose strikes correspond to 95, 100, and 105% of the current CDX spread.¹¹ CDX options in our data are based on the 5-year CDX. The sample period for

¹⁰Our estimation results are robust to using different proxies for the conditional SPX volatility. For instance, we obtain similar results when the conditional SPX volatility is estimated by smoothing realized variance measures based on high-frequency return time series.

¹¹For details on the pricing and market conventions about CDX options, we refer to Chen, Doshi, and Seo (2023) and Collin-Dufresne, Junge, and Trolle (2022).

CDX options starts in March 2012, which is when these contracts begin to trade in meaningful volumes.

3.2 Estimation strategy

In total, the model features 20 structural parameters and 2 latent variables. To reduce the dimensionality of the parameter space, we fix the values of some parameters following Feldhütter and Schaefer (2018) and Du, Elkamhi, and Ericsson (2019), among others. More precisely, we set the bankruptcy cost α to 25%, corporate tax rate ζ to 20%, and CDS/bond-specific recovery rate R to 51% when computing the protection leg of a CDS contract (see Appendix A). Considering our sample period, we choose the risk-free rate to be 1% and the asset payout ratio to be 2%. We normalize the amount of book liabilities to 25 and set the coupon c to $r \times 25 = 0.25$. Consistent with evidence that the default threshold is located significantly below the book value of liabilities, the default barrier A_D is chosen to be 78% of 25, or 19.50.¹²

In an attempt to further reduce the estimation dimensionality, we fix the idiosyncratic jump intensity λ_j to 1%, as simultaneously identifying the jump intensity and jump size is often challenging.¹³ This idiosyncratic jump intensity implies that, in expectation, about one idiosyncratic jump happens every 100 years per firm. Idiosyncratic jumps in the model are thus infrequent, but their size will be estimated to be very large, making a default highly likely when they occur. We also set the systematic jump intensity parameter η_m equal to $1/\theta$. Given that the physical jump intensity is defined by $\lambda_t^m = \eta_m V_t$, this value implies that about one systematic jump occurs on average per year. While idiosyncratic jumps are assumed to be rare in the model, systematic jumps on the other hand are assumed to be more frequent. This way, their expected size will be estimated to be less consequential for firms' defaults. Panel A of Table 1 summarizes and reports our calibration choices.

This leaves us with 11 structural parameters $\Theta \equiv \{\kappa, \theta, \delta, \rho, z_m, \gamma_m, \xi_{ALV}, \xi_V, \xi_m, \sigma_j, z_j\}$ to estimate and two latent variables (A_t^r, V_t) to filter. To do so, we adopt a daily observation

¹²This number is broadly consistent with the estimates in Davydenko (2012).

¹³Note that our assumed idiosyncratic jump intensity is of the same magnitude as the one in Collin-Dufresne, Junge, and Trolle (2022).

Panel A: Calibrated parameters	
1-Distress costs (α)	25.00%
2-Corporate tax rate (ζ)	20.00%
3-Recovery rate (R)	51.00%
4-Risk-free interest rate (r_f)	1.00%
5-Asset payout rate (q)	2.00%
6-Coupon (c)	0.25
7-Systematic jump intensity loading (η_m : $\lambda_t^m = \eta_m V_t$)	112.92
8-Idiosyncratic jump intensity (λ^j)	1.00%
9-Default barrier (A_D)	19.50
Panel B: Estimated parameters	
1-Mean reversion speed ($\hat{\kappa}$)	2.6637
2-Long run mean ($\hat{\theta}$)	0.0089
3-Volatility parameter for asset variance ($\hat{\delta}$)	21.49%
4-Correlation between asset value and variance shocks ($\hat{\rho}$)	-0.6004
5-Market price of asset specific risk ($\hat{\xi}_{A \perp V}$)	0.4759
6-Market price of variance risk ($\hat{\xi}_V$)	-6.1029
7-Systematic jump size mean (\hat{z}_m)	-3.24%
8-Systematic jump size standard deviation ($\hat{\gamma}_m$)	1.17%
9-Market price of systematic jump ($\hat{\xi}_m$)	-3.0010
10-Idiosyncratic volatility ($\hat{\sigma}_j$)	9.08%
11-Idiosyncratic jump size (\hat{z}_j)	-77.01%

Table 1: Structural parameters. The table reports the calibrated and estimated values for the structural model parameters. Panel A presents the parameters that are calibrated, and Panel B presents the parameters that are obtained via maximum likelihood estimation. The estimation sample period is from June 2004 to November 2020.

frequency and assume that the 5-year CDX spread ($S_{5,t}^{\text{CDX}}$) and the physical conditional SPX volatility (σ_t^{SPX}) are observed without errors (see, e.g., Duffee, 2002; Ait-Sahalia and Kimmel, 2010). We then filter out \hat{A}_t^r and \hat{V}_t from $S_{5,t}^{\text{CDX}}$ and σ_t^{SPX} , on each day t , by solving the following two equations:

$$S_{5,t}^{\text{CDX}} = S(\hat{A}_t^r, \hat{V}_t, 5, \Theta) \quad \text{and} \quad \sigma_t^{\text{SPX}} = \sqrt{\sigma_E^2(\hat{A}_t^r, \hat{V}_t, \Theta)}, \quad (15)$$

where S is defined by equation (10) and the expression for σ_E^2 is provided by

$$\sigma_{E,t}^2 = \left[\left(\frac{A_t^r}{E_t} \frac{\partial E_t}{\partial A_t^r} \right)^2 + \left(\frac{\delta}{E_t} \frac{\partial E_t}{\partial V_t} \right)^2 + 2\rho\delta \frac{A_t^r}{(E_t)^2} \frac{\partial E_t}{\partial A_t^r} \frac{\partial E_t}{\partial V_t} \right] V_t + \lambda_t^m \mathbb{E}_{Z^m} \left[\frac{E(A_t^r e^{Z_t^m}, V_t)}{E_t} - 1 \right]^2.$$

We provide the detailed derivation in the Internet Appendix. On the one hand, risk-neutral

pricing implies that the term structure of CDX spreads embeds relevant information about the model's \mathbb{Q} -dynamics. On the other hand, the time series of the conditional SPX volatility and CDX spreads help us identify the model's \mathbb{P} -dynamics. Since there are inherent differences in the payoffs of the claims constituting the SPX and CDX, diffusive and jump risks impact the pricing of credit and equity indices differently. Thus, fitting the CDX level jointly with the physical SPX volatility is not only informative about \mathbb{P} - and \mathbb{Q} -dynamics but also about the decomposition of the total asset risk into its respective components.

Our estimation strategy further postulates that the relative pricing errors on 3-, 7-, and 10-year CDX spreads are observed with Gaussian errors such that

$$\frac{S_{T,t}^{\text{CDX}} - S(A_t^r, V_t, T, \Theta)}{S_{T,t}^{\text{CDX}}} = e_{T,t}, \quad \text{for } T = 3, 7, 10, \quad (16)$$

where $S_{T,t}^{\text{CDX}}$ is the T -year maturity quoted spread at time t and $e_{T,t} \sim N(0, \sigma_e^2)$. Based on these assumptions, we estimate Θ via maximum likelihood by solving the following maximization problem

$$\hat{\Theta} \equiv \operatorname{argmax} \log \mathcal{L}(\Theta) = \operatorname{argmax} \sum_{t=2}^T \log \mathbb{P}(Y_t | Y_{t-1}; \Theta), \quad (17)$$

where $Y_t = \{S_{3,t}^{\text{CDX}}, S_{5,t}^{\text{CDX}}, S_{7,t}^{\text{CDX}}, S_{10,t}^{\text{CDX}}, \sigma_t^{\text{SPX}}\}$ is the vector of observables on day t . Note that the distribution of the filtered state variables and the mapping from $\{\hat{A}_t^r, \hat{V}_t\}$ to the vector of observables Y_t are taken into account when computing $\mathbb{P}(Y_t | Y_{t-1}; \Theta)$. Details about the construction and computation of the likelihood function in our framework are provided in the Internet Appendix.

3.3 Parameter estimates

Panel B of Table 1 presents the 11 structural parameters that are obtained via maximum likelihood estimation following the strategy outlined in the previous section. The first four rows of Panel B report the parameters governing systematic asset variance dynamics. The estimated mean reversion speed ($\hat{\kappa}$) is 2.6637. This value corresponds to a daily persistence of

$1 - 2.6637/365 = 0.9927$, which is comparable to the persistence of variance reported for large equity indices (see, e.g., Bates, 2000; Pan, 2002). The long-run mean of systematic variance $\hat{\theta}$ is 0.0089, which translates into a yearly volatility level of $\sqrt{0.0089} = 9.41\%$.

The volatility of variance parameter is 21.49% and the correlation $\hat{\rho}$ between the two systematic Brownian motions $W_t^{A\perp V}$ and W_t^V is -0.6004. Apart from the level of systematic asset variance, which is lower than that of an equity index due to the firms' financial leverage, the remaining estimates for systematic asset variance are comparable to the parameters reported in Bates (2000), Pan (2002), and Christoffersen, Fournier, and Jacobs (2018) for the dynamics of the SPX variance.

The next two parameters reported in rows 5-6 capture diffusive risk compensation. The estimated market price of asset diffusive risk ($\hat{\xi}_{A\perp V}$) is equal to 0.4759 while the market price of variance risk ($\hat{\xi}_V$) is -6.1029. Combined, $\hat{\rho}$, $\hat{\xi}_{A\perp V}$, and $\hat{\xi}_V$ imply that the estimated risk premium attributable to diffusive risk is $\left(\sqrt{1 - \hat{\rho}^2} \hat{\xi}_{A\perp V} + \hat{\rho} \hat{\xi}_V\right) V_t = 4.0449 \times V_t$ in equation (7). Unconditionally, this translates to $4.0449 \times \hat{\theta} = 3.58\%$ annually. Moreover, the estimated risk-neutral mean reversion speed and unconditional variance are $\hat{\kappa}^{\mathbb{Q}} = \hat{\kappa} + \hat{\delta} \hat{\xi}_V = 1.3522$ and $\hat{\theta}^{\mathbb{Q}} = \hat{\kappa} \hat{\theta} / \hat{\kappa}^{\mathbb{Q}} = 0.0174$, respectively. The negative $\hat{\xi}_V$ estimate thus translates into a more persistent variance process and a higher unconditional level of variance under \mathbb{Q} than under \mathbb{P} . This finding is consistent with a wealth of evidence on the presence of a negative variance risk premium.¹⁴

The parameters reported in rows 7-9 in Panel B govern the systematic jump distribution and the market price of systematic jump risk. The mean (\hat{z}_m) and volatility ($\hat{\gamma}_m$) of systematic jumps are -3.24% and 1.17%, respectively. The market price of systematic jump risk $\hat{\xi}_m$ is negative and equals -3.0010. This estimate implies that the average systematic jump size is more negative under \mathbb{Q} than under \mathbb{P} . We have $\hat{z}_m^{\mathbb{Q}} = \hat{z}_m + \hat{\xi}_m \hat{\gamma}_m^2 = -3.28\%$.¹⁵ In terms of contribution to the total asset risk premium ($\mu_t - r$), the unconditional systematic jump

¹⁴See, among many others, Carr and Wu (2009) or Todorov (2010).

¹⁵The systematic jump intensity $\lambda_t^{m,\mathbb{Q}} = \eta_m^{\mathbb{Q}} V_t$ is also higher under the risk-neutral measure. There are two reasons. First, the risk-neutral loading $\eta_m^{\mathbb{Q}} = \eta_m e^{\xi_m z_m + \frac{1}{2}(\xi_m)^2 \gamma_m^2}$ is larger than the physical loading η_m (124.51 vs. 112.92). Second, the level of V_t under the risk-neutral measure $\theta^{\mathbb{Q}} = \kappa \theta / (\kappa + \delta \xi_V)$ is larger than its physical counterpart θ (1.352 vs. 0.0089).

component, obtained by setting λ_t^m to $\hat{\eta}_m \hat{\theta}$ in $\lambda_t^m \mathbb{E}[(1 - e^{Z_t^m})(e^{\xi_m Z_t^m} - 1)]$, is equal to 0.37%. This number amounts to a 9.37% relative contribution to the total asset risk premium of $(3.58\% + 0.37\%) = 3.95\%$. Finally, in rows 10-11, we report two idiosyncratic/firm-specific parameters. The estimated diffusive idiosyncratic volatility $\hat{\sigma}_j$ is 9.08% and the estimated idiosyncratic jump size \hat{z}_j is -77.01%.

A well-known shortcoming of a misspecified structural model is that it implies an excessive asset Sharpe ratio or market leverage when it is estimated to fit the data (in particular, the credit spread). In the same spirit, the estimated level of asset volatility gains economic relevance only if the model implies a reasonable asset Sharpe ratio and market leverage; a low level of asset volatility could be compensated by excessive leverage or other sources of risk, leading to an unrealistically large asset Sharpe ratio. Thus, it is important to check if the two aforementioned measures are reasonable in our model. First, the asset Sharpe ratio of the representative firm is 23% under our parametrization, which compares well with other values reported in the literature. For instance, Chen, Collin-Dufresne, and Goldstein (2009) discuss the importance of the asset Sharpe ratio in structural models and obtain a 22% asset Sharpe ratio estimate for a representative Baa firm. Second, the market leverage of the representative firm implied by the model is 44.18%, which is of the same order of magnitude as the empirical estimates for our sample of firms. According to Choi, Doshi, Jacobs, and Turnbull (2019), the market leverage of CDX firms, measured as the ratio of total liabilities (Compustat item LTQ) to market equity plus total liabilities, ranges from 44.90% to 63.10% on average across firms. These results establish consistency between our model and the data and provide further confidence in our estimated parameters.

4 Understanding the model mechanisms

Before presenting the filtered state variables and discussing the model's time series implications, we seek to provide insights into the mechanisms at play in our model. We first examine the relation between the state variables and key model quantities (Section 4.1). We then study how the exposures to the three sources of systematic risk vary across indices and derivative

instruments (Section 4.2). Lastly, we show that our estimated model can consistently price the CDX, SPX options, and CDX options, addressing the puzzle posed by Collin-Dufresne, Junge, and Trolle (2022) (Section 4.3).

4.1 The role of the state variables

Equipped with the parameter estimates from Section 3, we evaluate the model at various combinations of the state variables (A_t^r, V_t) to understand how it operates. In our model, the first state variable A_t^r is only identified up to its ratio with the default barrier A_D . So we select the following levels for the relative default barrier:

$$\frac{A_D}{A_t^r} \in \left\{ 0.35022, 0.38298, 0.49218 \right\}.$$

The three values above are selected based on empirical estimates of market leverage. Specifically, the lower value of 0.35022, the mid value of 0.38298, and the upper value of 0.49218 correspond to 78% of the lower bound, time series mean, and upper bound of the average market leverage for CDX firms documented by Choi, Doshi, Jacobs, and Turnbull (2019).

We also choose three values of the second state variable V_t based on its stationary distribution under the physical measure:

$$V_t \in \left\{ 0.00097, 0.00619, 0.02028 \right\},$$

which correspond to the 10th, 50th (median), and 90th percentile values. Note that since V_t follows a Cox, Ingersoll, and Ross (1985) process, its stationary distribution is gamma with shape parameter $2\kappa\theta/\delta^2$ and scale parameter $\delta^2/(2\kappa)$.

We calculate the 5-year CDX spread as well as 1-month SPX/CDX implied volatilities based on the $3 \times 3 = 9$ pairs of the state variables. Table 2 reports the results obtained. Panel A shows that the CDX spread sharply increases with the relative default barrier. At the median V_t , the CDX spread is only 43.78 bp for the low level of A_D/A_t^r but rises to 64.36 bp and to 148.64 bp for the mid and high values. This is intuitive. A higher default

barrier corresponds to a shorter distance to default, leading to a larger default probability and CDX spread. We observe that the CDX spread is also monotonically increasing with asset variance V_t independently of the level of the relative default barrier. If the asset dynamics become more volatile, the asset value is more likely to hit the default barrier and trigger a default. Consistent with this intuition, for the middle value of A_D/A_t^r , the CDX spread goes up from 58.38 to 73.71 as V_t moves from its lowest to highest decile.

		(A) CDX	(B) SPX options			(C) CDX options		
			95%	100%	105%	95%	100%	105%
Low relative default barrier A_D/A_t^r								
V_t	10th	41.65	10.01	6.48	5.97	21.55	26.01	29.84
	Median	43.78	15.50	13.13	11.14	48.59	51.62	54.12
	90th	50.67	24.81	23.19	21.69	84.98	86.12	86.91
Mid relative default barrier A_D/A_t^r								
V_t	10th	58.38	10.38	6.81	6.18	22.49	27.73	31.53
	Median	64.36	16.21	13.81	11.76	46.85	48.75	50.29
	90th	73.71	26.07	24.40	22.87	72.06	72.71	73.27
High relative default barrier A_D/A_t^r								
V_t	10th	141.38	11.97	8.26	7.31	15.13	19.64	23.00
	Median	148.64	19.33	16.78	14.57	32.65	35.32	37.59
	90th	161.89	31.49	29.66	27.96	55.80	58.19	60.19

Table 2: Model results as functions of the state variables. The table reports the 5-year CDX spread (Panel A) and 1-month SPX and CDX implied volatilities (Panels B and C) from the model. We evaluate the model at the following nine combinations of the two state variables: $(\frac{A_D}{A_t^r}, V_t) \in \{0.35022, 0.38298, 0.49218\} \times \{0.00097, 0.00619, 0.02028\}$. The CDX spread is expressed in basis points. The SPX and CDX implied volatilities are calculated at the 95, 100, and 105% moneyness values and are expressed in percentages.

Panel B finds similar monotonic patterns for the SPX implied volatility, which unambiguously rises with both state variables. In a structural credit risk model, equity is a residual claim on the issuing firm’s asset. Thus, both higher asset variance and financial leverage translate into higher equity volatility. If financial leverage (equivalently, the relative default barrier) rises, the sensitivity of the equity to assets increases, making the equity return more volatile. This, in turn, makes equity options more valuable, as reflected in the increasing patterns of the SPX implied volatility. Additionally, our model generates a pronounced negative volatility skew consistent with empirical stylized facts; at any given combination of the two state variables, the SPX implied volatility decreases with moneyness (K/I_t). The negative skewness

in SPX returns, which results in a downward sloping implied-volatility skew, is induced by: (i) asymmetric asset volatility generated through a negative correlation coefficient ρ and (ii) downward systematic asset jumps $\nu_t^m dN_t^m$. In addition, the asymmetry in unlevered asset risk implied by (i) and (ii) endogenously generates a higher market leverage of constituting firms in bad times, further increasing index volatility in the left tail.

Panel C, however, presents quite different patterns for the CDX implied volatility. A few remarks are in order. First, the model generates a positive volatility skew. Intuitively, a left tail event in the equity market (low equity return) is associated with a right tail event in the credit market (high credit spread). Hence, a downward sloping volatility skew for SPX options is consistent with an upward sloping volatility skew for CDX options. Second, the CDX implied volatility does not vary monotonically with the relative default barrier A_D/A_t^r . For example, for the low V_t value, at-the-money volatilities display a hump-shaped pattern (26.01, 27.73, and 19.64 bp) as A_D/A_t^r increases.

To understand this, it is important to note that the CDX implied volatility captures the volatility of the relative change in the CDX spread through the Black (1976) formula. Thus, all else equal, the CDX implied volatility tends to decline when the level of the CDX spread rises. Simply put, a 40 bp standard deviation in the CDX spread corresponds to a 100% volatility when the CDX spread is 40 bp but corresponds to a 50% volatility when the CDX spread is 80 bp. This makes it clear that the hump-shaped pattern is the result of two opposite forces. (i) On the one hand, higher market leverage leads to higher default risk, raising the CDX implied volatility. (ii) On the other hand, higher market leverage boosts the level of the CDX spread, decreasing the CDX implied volatility. Depending on which force dominates the other, the CDX implied volatility can go up or down.

Interestingly, we do not observe any non-monotonicity when changing V_t for a given relative default barrier: the CDX implied volatility always rises with asset variance V_t , similar to the SPX implied volatility case. When we increase asset variance, the CDX spread rises with a relatively small magnitude (Panel A). As a result, the negative force (through the spread level) is always dominated by the positive force, preserving the monotonicity in the CDX implied

volatility along V_t .

4.2 Heterogeneity in systematic risk exposures

In our model, the expected return on a given corporate security is determined by the product of aggregate risk premia times its risk exposures (see equation (14)). As a result, cross-sectional differences in expected returns are entirely driven by heterogeneity in the three systematic risk exposures $\Delta_{A,t}$, $\Delta_{V,t}$, and $\Delta_{N,t}$ across different securities. In this section, we develop economic insights into how these exposures differ across the two market indices and their option contracts.

To estimate exposures for the CDX, we consider a fully collateralized contract from the protection seller's point of view. In this case, the value of the CDX contract is equivalent to the value of a synthetic corporate bond (Chen, Doshi, and Seo, 2023). Putting down the collateral corresponds to paying for the bond, the premium leg captures the value of receiving a credit spread on the bond, and the protection leg reflects the loss in the event of default. In what follows in this section, we refer to this fully collateralized CDX position when we use the term CDX or CDX value. See Appendix A for details.

Figure 1 graphs the exposures to the three sources of risk implied by the model for the SPX/CDX (Panels A, B, and C), for SPX options (Panels D, E, and F), and for CDX options (Panels G, H, and I). For both types of options, we consider 1-month calls and puts with moneyness of 95, 100, and 105%. To facilitate comparison, we normalize the exposures so that they capture the response to a one standard deviation change in one of the three sources of systematic risk. Specifically, the left panels plot the normalized asset risk exposure $\Delta_{A,t} \times \text{Std}_t\left(\frac{dA_t}{A_t}\right) = \Delta_{A,t}\sqrt{V_t}$, the center panels plot the normalized variance risk exposure $\Delta_{V,t} \times \text{Std}_t(dV_t) = \Delta_{V,t}\delta\sqrt{V_t}$, and the right panels plot the normalized jump risk exposure $\bar{\Delta}_{N,t} \times \text{Std}_t(dN_t) = \bar{\Delta}_{N,t}\sqrt{\lambda_t^m}$. The results are produced by setting the two state variables ($A_D/A_t^r, V_t$) to their mid values selected in Section 4.1.

Panel A shows that the SPX and CDX values are both positively exposed to asset growth risk. This is intuitive. When the firm's asset value increases (i.e., $\partial A_t^r/A_t^r > 0$), equity (SPX)

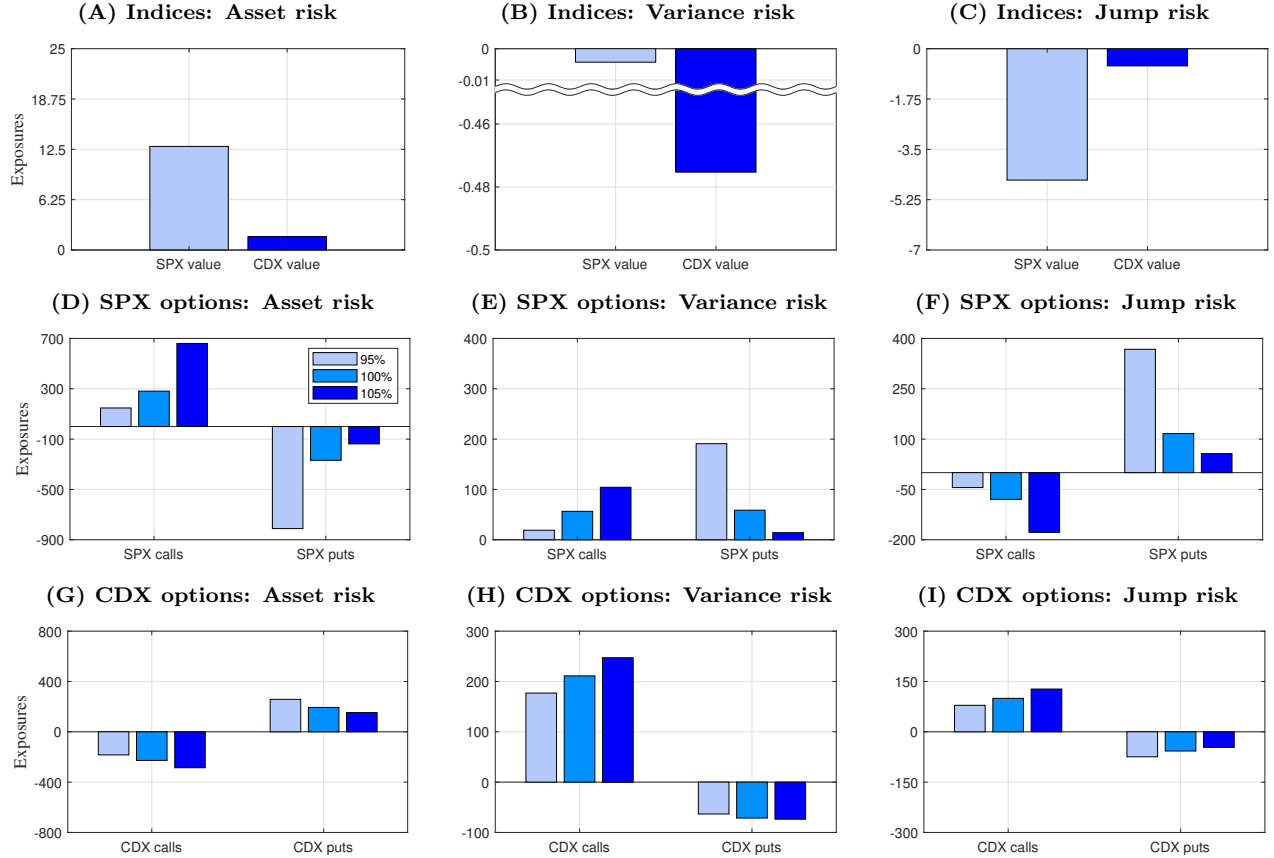


Figure 1: Exposures to three sources of systematic risk. The figure graphs the three exposures implied by the model for the SPX/CDX (Panels A, B, and C), for SPX options (Panels D, E, and F), and for CDX options (Panels G, H, and I). For both types of options, we consider 1-month calls and puts with moneyness of 95, 100, and 105%. To facilitate comparison, we normalize the exposures so that they capture the response to a one standard deviation change in one of the three sources of systematic risk. Specifically, the left panels plot $\Delta_{A,t}\sqrt{V_t}$, the center panels $\Delta_{V,t}\delta\sqrt{V_t}$, and the right panels $\bar{\Delta}_{N,t}\sqrt{\lambda_t^m}$. The results are produced by setting the two state variables at $(A_D/A_t^r, V_t) = (0.38298, 0.00619)$.

and debt (CDX), both claims on the firm’s assets, should also increase in value. Notably, the SPX has a greater exposure than the CDX. This is due to inherent disparities in cash flow contingencies between equity vs. debt; equity is a more junior claim than debt, offering more upside and embedded leverage.

Moving on to options, we observe from Panel D that SPX calls load positively and SPX puts load negatively on asset growth risk, as expected. We also find that out-of-the-money options (105% for calls and 95% for puts) have generally larger exposures than at-the-money or in-the-money options because of their higher embedded leverage. For CDX options in Panel G, intuitively, calls load negatively and puts load positively on asset growth risk. Since

the credit spread generally rises in bad times and falls in good times, CDX calls (puts) are similar to SPX puts (calls) with respect to the economic states they span.

The exposures to jump risk in Panels C, F, and I present the exact opposite signs to those for asset growth risk. This is because systematic jumps are on average negative in our model, reducing the firm’s asset value. Naturally, the exposure to jump risk $\bar{\Delta}_{N,t}$ takes the opposite sign compared to $\Delta_{A,t}$. Therefore, while the SPX still has a greater exposure in magnitude than the CDX, both are negatively exposed. SPX calls and CDX puts load negatively on jump risk whereas SPX puts and CDX calls load positively.

An intriguing prediction of our model is that exposures to variance risk $\Delta_{V,t}$ vary, both in size and sign, across markets and instruments. In Panel B, we see that the exposure of the CDX to variance risk is significantly larger in magnitude than that of the SPX, although both are negative. Why do the two indices exhibit such a drastic difference in exposures? There are two channels at play here. (i) When asset variance V_t rises, investors’ marginal utility or the SDF goes up. Consequently, the values of corporate securities, whose cash flows are lower in bad times when V_t is high, decline. Thus, under this channel, equity and debt values fall together. (ii) In a structural credit risk model like ours, corporate securities are implicitly option contracts on the firm’s assets: equity is a long call whereas debt embeds a short put. When asset variance V_t rises, the value of an option, regardless of whether it is a call or a put, also rises as the chance of expiring in-the-money increases. This so-called “vega effect” raises the equity value (i.e., long call) but lowers the debt value (i.e., short put).

As a result, the exposures of the SPX and CDX to variance risk in Panel B are determined by the net effect of these two channels. In the case of the SPX, which is an equity index, channels (i) and (ii) have opposite effects, partially offsetting each other. At the given state variables, channel (i) slightly dominates channel (ii), leading to a marginally negative exposure. However, in the case of the CDX, which is based on debt securities, channels (i) and (ii) go in the same direction, making the CDX exposure heavily negative. The CDX is thus much more sensitive to variance risk than the SPX.

Understanding the intuition behind Panel B, it is clear how the exposures of options to

variance risk in Panels E and H are determined. Again, we need to consider the interplay of two channels. Starting with SPX options in Panel E, consider a situation where asset variance V_t rises. On the one hand, the value of the underlying (i.e., SPX) slightly falls, as can be seen in Panel B, making SPX calls less valuable and SPX puts more valuable (underlying channel). On the other hand, an increase in asset variance leads to an increase in SPX variance, and due to the associated vega effect, both SPX calls and puts become more valuable (vega channel). The underlying channel is weak for the SPX and is dominated by the vega channel. This explains why we have positive exposures to variance risk for all SPX options.

In contrast, Panel H reveals that CDX calls and puts carry exposures with opposite signs. Specifically, the exposures of CDX puts turn negative. To illustrate why, recall that the value of the CDX falls more substantially than the SPX in Panel B. This implies that for CDX options, the underlying channel can dominate the vega channel, depending on the contract. For CDX calls, when asset variance V_t rises, the CDX value falls, and equivalently, the CDX spread rises. Thus, both the underlying and vega channels go in the same direction, making CDX calls heavily and positively exposed to variance risk. For CDX puts, the underlying channel reduces the put value and goes against the vega channel. In fact, for CDX puts, the underlying channel dominates the vega channel under our parametrization, resulting in negative exposures, as can be seen in Panel H.

Comparing the magnitudes of at-the-money exposures to variance risk, we see that CDX calls offer the largest exposures among all options by an order of magnitude. Thus, although CDX put options are negatively exposed to variance risk, the substantially large positive exposures of CDX calls imply that selling at-the-money CDX straddles can generate high average returns. This rationalizes the empirical finding documented by Collin-Dufresne, Junge, and Trolle (2022) that selling at-the-money CDX straddles produce much higher returns than selling at-the-money SPX straddles.¹⁶ The key economic intuition is clear. As evident in Panel B, the CDX is simply more sensitive to variance risk than the SPX.

¹⁶Shorting straddles, or selling volatility insurance, generates a positive premium arising from a negative exposure to (negatively priced) variance risk. Our model predicts that CDX straddle returns should be about twice as high as SPX straddle returns. This is broadly in line with the empirical ratio between the two returns in their paper.

4.3 Comparison with Collin-Dufresne, Junge, and Trolle (2022)

An important aspect of our model is that it can shed light on the puzzle documented by Collin-Dufresne, Junge, and Trolle (2022) (henceforth, CJT in this section). CJT argue that even with a state-of-the-art structural model of credit risk, it is difficult to reconcile the pricing of SPX and CDX options simultaneously. Specifically, they find that when their model is fitted to match the CDX spread and implied volatilities for SPX options, it generates too low implied volatilities for CDX options.¹⁷ Based on this inherent inconsistency between the two types of option contracts, CJT conclude that equity and credit option markets are not fully integrated.

Before we investigate this issue through the lens of our model, it is worth highlighting that our paper takes a different empirical approach compared to CJT. In our model, we specify both the physical and risk-neutral firm dynamics and estimate them not only by using the risk-neutral information from asset prices but also by exploiting the physical information embedded in the time series. The state variables are filtered so as to preserve the assumed dynamics of our model. In contrast, CJT exclusively model risk-neutral dynamics; the model state variables are treated as extra parameters and fitted to asset prices along with other parameters every 6 months. In this section, we revisit the fitting exercise in the spirit of CJT using our model. The formal empirical results based on the filtered state variables are provided in Section 5.

Table 3 shows the results from our fitting exercise. In Panel A, we report the data median for the CDX spread as well as for the at-the-money SPX and CDX implied volatilities. The sample period is from March 2012 to November 2020, during which the data on both options are available. In Panel B, we search for the values of the two state variables so that our estimated model generates the same CDX spread (67.50 bp) and SPX implied volatility (13.27%) as in the data. The fitted values of the state variables are $(A_D/A_t^r, V_t) = (0.3880, 0.0056)$, which are within the range discussed in Section 4.1. Surprisingly, the panel shows that our model, together with the fitted state variables, implies a CDX implied volatility of

¹⁷Equivalently, when their model is fitted to match the CDX spread and implied volatilities for CDX options, it implies too high implied volatilities for SPX options.

	CDX	Implied volatility		Model inputs		
		SPX	CDX	A_D/A_t^r	V_t	σ_j
(A) Data median (Mar 2012 - Nov 2020)	67.50	13.27	41.74			
(B) Our benchmark parametrization	67.50	13.27	46.35	0.3880	0.0056	0.0980
+ (1) Lower A_D/A_t^r but higher σ_j	67.50	9.90	25.83	0.1712	0.0056	0.3204
+ (2) Higher asset variance V_t	67.50	13.42	32.43	0.1712	0.0108	0.3178
+ (3) Other changes to reach CJT	67.50	13.27	33.44	0.1712	0.0108	0.2840
(C) CJT parametrization	67.50	13.27	33.44	0.1712	0.0108	0.2840

Table 3: Pricing consistency. The table revisits the relative pricing puzzle posed by CJT based on our model. Panel A reports the data median for the CDX spread as well as for the at-the-money SPX and CDX implied volatilities. The sample period is from March 2012 to November 2020, during which the data on both options are available. The other two panels calculate the CDX implied volatility from the model when the two state variables are chosen to exactly fit the CDX spread and the SPX implied volatility from the data under our benchmark parametrization (Panel B) and under CJT’s parametrization (Panel C). Reported together are three key model inputs. To understand why the two parametrizations produce different results, in Panel B, we begin with our benchmark parametrization and gradually change the values of the parameters and state variables until we reach CJT’s parameterization.

46.35%. The model value is close to and even slightly larger than the data value of 41.74%. Unlike the findings of CJT, the model does not underprice CDX options under our benchmark parametrization, although the model is fitted to perfectly match the CDX spread and SPX implied volatility.

Why don’t we reproduce the relative pricing puzzle posed by CJT? Our model differs from CJT’s in two dimensions. First, the two models make different assumptions about capital structure and firms’ defaults. In our model, firms issue console bonds and go bankrupt when the asset value falls below an exogenously specified default boundary (i.e., first-passage-time model in the spirit of Black and Cox, 1976). In CJT’s model, however, firms maintain a lumpy debt structure by issuing a 1-year short-term bond and a 5-year longer-term bond. At year 1, the default boundary is endogenously determined based on the continuation value of equity. At year 5, the default boundary is simply set to be the face value of the 5-year bond as in the standard Merton (1974) setup. Despite these differences, the two models are still comparable because they share identical asset dynamics with stochastic variance and jump risks. In fact, we are able to map the parameters associated with firms’ asset dynamics under CJT’s model exactly into ours. This naturally points toward the second difference between the two models: parameter values.

To understand the impact of differences in parametrization, Panel C now evaluates our model with the parameters reported by CJT.¹⁸ Like in Panel B, the values of the two state variables are found to match the CDX spread and SPX implied volatility. In this case, the model leads to only a 33.44% CDX implied volatility, nearly 10% points (or 20% in relative terms) lower than the data. Hence, we do recover the underpricing issue documented by CJT if we use their parametrization.¹⁹

Then, why do the two parametrizations deliver such different results? In Panel B, we begin with our benchmark parametrization and gradually change the values of the parameters and state variables until we reach CJT’s parameterization. Most noticeably, CJT adopt a larger idiosyncratic volatility σ_j (28.40% vs. 9.80%) but instead a lower relative default threshold A_D/A_t^r (0.1712 vs. 0.3880). In row (1) of Panel B, we set A_D/A_t^r to 0.1712 and increase σ_j to match the CDX spread. Although the total credit risk remains the same (i.e., identical CDX spread), the proportion of idiosyncratic (diversifiable) risk rises. Consequently, the implied volatilities for both index options fall significantly. In row (2) of Panel B, we additionally raise the asset variance V_t from 0.0056 to 0.0108, the average systematic variance reported in CJT. At the same time, we slightly lower σ_j to keep the CDX spread unaffected. We observe that the SPX implied volatility goes up to 13.42% as a result, returning to the data level. However, the CDX implied volatility, at 32.43%, remains lower than the data value of 41.74%. Note that row (2) already closely replicates the results from the CJT parametrization in Panel C. In fact, other parameter differences, such as the frequency/severity of jumps or persistence/long-run mean of asset variance, cancel one another and generate little net effect.

This exercise demonstrates that jointly explaining the pricing of the CDX, SPX options, and CDX options requires the right balance between different sources of risk. There are two tensions to be considered. The first tension is between systematic risk and idiosyncratic risk.

¹⁸Since they estimate their model every 6 months, we use the average parameter estimates. Also, note that CJT only specify risk-neutral dynamics, and their parameters should be interpreted as risk-neutral ones. We correctly map their parameters into the risk-neutral parameters of our model. The Internet Appendix reports the CJT parameters used in this exercise along with our benchmark parametrization for comparison purposes.

¹⁹This degree of underpricing is somewhat smaller than what CJT report (around 30% in relative terms). This small discrepancy could potentially be due to (i) other differences between the two models such as capital structure and default assumptions, or (ii) larger model pricing errors outside of “average” market conditions.

The relative contribution of systematic vs. idiosyncratic risk does not affect the level of the CDX spread, as it only depends on the total risk of the constituent firms. However, through diversification, this relative contribution matters for index dynamics and therefore influences index option prices. The second tension comes from different origins of systematic risk. As explored in Section 4.2, asset risk, variance risk, and jump risk have differential impacts on SPX and CDX options. Therefore, depending on their relative contributions, the three sources of systematic risk can lead to different pricing implications.

5 Empirical analysis

The empirical evaluation of our model’s goodness-of-fit is composed of three parts. In Section 5.1, we examine the model’s in-sample fit for the term structure of CDX spreads and the conditional SPX volatility. We then turn to the out-of-sample analysis. In Section 5.2, we analyze the performance of the model in jointly explaining the pricing of SPX and CDX options. Model implications for expected option returns and risk premia are discussed in Section 5.3.

5.1 In-sample fit

Recall that we filter the state variables from the 5-year CDX spread ($S_{5,t}^{\text{CDX}}$) and the physical SPX volatility (σ_t^{SPX}) by solving $S_{5,t}^{\text{CDX}} = S(\hat{A}_t^r, \hat{V}_t, 5, \hat{\Theta})$ and $\sigma_t^{\text{SPX}} = \sqrt{\sigma_E^2(\hat{A}_t^r, \hat{V}_t, \hat{\Theta})}$ for \hat{A}_t^r and \hat{V}_t . Figure 2 presents the filtered time series of the relative default barrier A_D/\hat{A}_t^r and systematic asset variance \hat{V}_t backed out by our estimation procedure. From the figure, we see that the two state variables behave as expected. The asset value \hat{A}_t^r displays procyclical patterns, making the relative default barrier A_D/\hat{A}_t^r in Panel A countercyclical. Panel B shows that the filtered asset variance \hat{V}_t also displays countercyclicity. Notably, the relative default barrier rises at the onset of the Global Financial Crisis. Around the same period, asset variance increases abruptly, reflecting the adverse economic climate during the crisis; the 5-year CDX spread increased as high as 250 bp and the SPX volatility shot up to nearly 75%. In 2020, we observe similar patterns for the two state variables at the beginning of the

COVID-19 crisis, which is sensible.

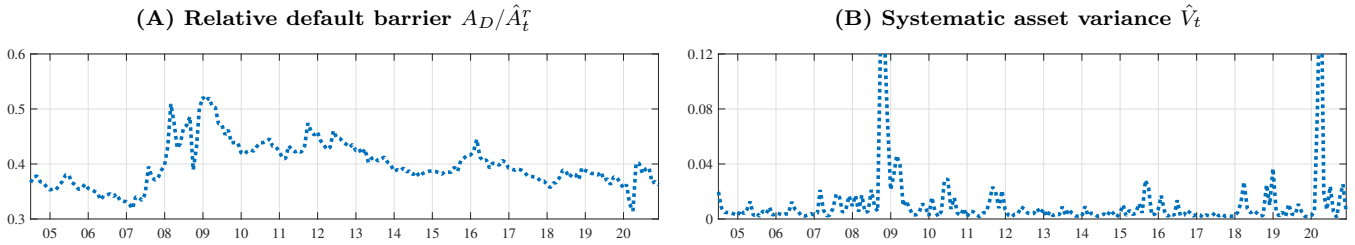


Figure 2: Filtered state variables. The figure presents the time series of the two filtered state variables: the relative default barrier A_D/\hat{A}_t^r (Panel A) and systematic asset variance \hat{V}_t (Panel B). The measurement frequency is monthly, where the values of the two filtered state variables are sampled at the end of each month. The sample period is from June 2004 to November 2020.

We now examine the in-sample fit of our model implied by the filtered state variables and parameter estimates. In Figure 3, we plot the time series of the 3-, 5-, 7-, and 10-year CDX spreads and the physical SPX volatility in the data (yellow solid lines) and in the model (blue dotted lines). Since the model is estimated to exactly match the 5-year CDX spread and the SPX volatility, the data and model series perfectly coincide for these two variables in Panels B and E. Thus, the main variables of interest to assess the quality of in-sample model fit are the CDX spreads with 3-, 7-, and 10-year maturities. Panels A, C, and D show that the model captures time variation in the CDX spreads well for these maturities. The figure reveals that most pricing errors cluster around the Global Financial Crisis period, which is not surprising. Outside of this period, the model tracks the data quite closely.

More formally, Panels A and B of Table 4 compare the means and standard deviations of the variables calculated from the data and model. From Panel A, we see that the empirical term structure of CDX spreads is upward sloping on average. The spread monotonically rises from 56.25 bp for the 3-year maturity to 108.45 bp for the 10-year maturity. Another interesting observation is that long-term spreads are less volatile than short-term spreads. While the standard deviation is 42.66 bp for the 3-year maturity, the 10-year spread has a volatility of 25.95 bp. Our model captures these stylized facts relatively well, as can be seen from Panel B. The model implied averages and standard deviations are close to their data counterparts. The 3-year CDX spread is 48.84 bp on average in the model, which is slightly lower than the empirical average of 56.25 bp. For the long end of the term structure, the

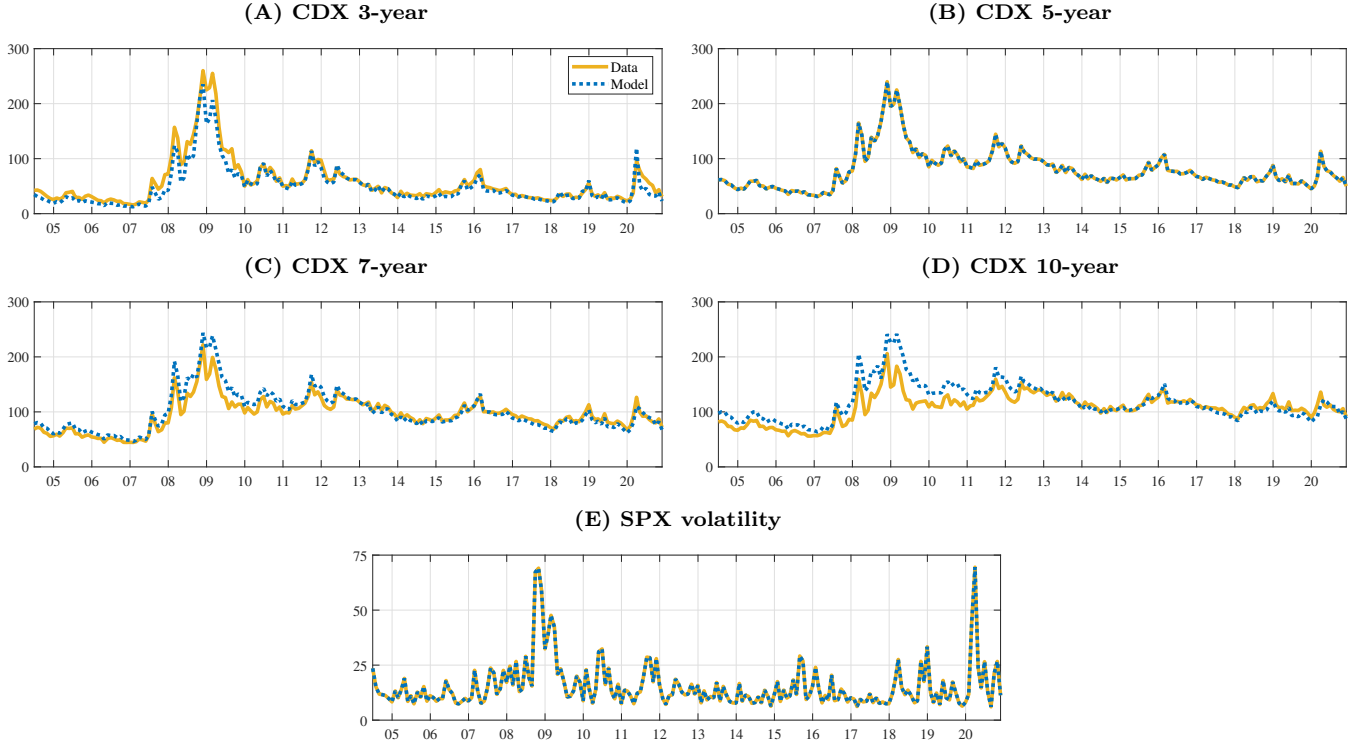


Figure 3: CDX spreads and SPX physical volatility. The figure plots the monthly time series of the 3-, 5-, 7-, and 10-year CDX spreads and the physical SPX volatility in the data (yellow solid lines) and in the model (blue dotted lines). The CDX spreads are expressed in basis points. The SPX volatility is expressed in percentages. The sample period is from June 2004 to November 2020.

model values are slightly higher than in the data (e.g., 118.37 vs. 108.45 bp for the 10-year maturity). In terms of standard deviations, the model estimates are of the same order of magnitude as the empirical values, but their term structure is somewhat flatter in the model than in the data.

To provide further insight into our model’s goodness of fit, Panel C of Table 4 provides two diagnostic metrics: the correlation between the data and the model as well as the root mean square error (RMSE). First of all, the data and model series are highly correlated. The correlation estimates range from 0.86 to 0.97, which indicates that the model is able to capture time series fluctuations well. In terms of pricing errors, the RMSE estimates range from 12.68 to 20.11 bp. Considering the structural nature of our approach, these estimates are reasonable and comparable to the magnitude of pricing errors reported in the literature.²⁰

²⁰Unlike reduced-form frameworks where price dynamics are exogenously specified to fit the data best, our structural approach is relatively less flexible, as price dynamics are endogenously determined from the firm’s asset dynamics.

	(A) Data		(B) Model		(C) Fit	
	Mean	Std.	Mean	Std.	Corr.	RMSE
CDX 3-year	56.25	42.66	48.84	36.31	0.97	13.23
CDX 5-year	79.85	35.77	79.85	35.77	–	–
CDX 7-year	94.93	29.62	99.83	36.48	0.96	12.68
CDX 10-year	108.45	25.95	118.37	33.91	0.86	20.11
SPX volatility	15.46	10.40	15.46	10.40	–	–

Table 4: In-sample model goodness of fit. The table examines the in-sample model goodness of fit. Panels A and B report the sample means and standard deviations of the 3-, 5-, 7-, and 10-year CDX spreads and the physical SPX volatility in the data and in the model. In Panel C, we present two goodness of fit metrics to assess model performance: the time-series correlation between the data and the model as well as the root mean squared error (RMSE). The measurement frequency is monthly, where the data and model values are sampled at the end of each month. The sample period is from June 2004 to November 2020.

It is worth emphasizing that our in-sample results are only meaningful if the model implies reasonable \mathbb{P} -dynamics for defaults. If the model were to generate large CDX spreads while predicting excessively high physical default probabilities, then, the model would fall into the trap of the credit spread puzzle. In-sample, the average 10-year cumulative physical default probability generated by the model is 4.55%, which is close to the historical 10-year default rate for the Baa grade entities reported in Moody’s credit report (3.70% for 1970-2018 and 5.50% for 1920-2018). This result, combined with the fact that the fitted asset Sharpe ratio and market leverage are reasonable (see Section 3.3), provides evidence that our model is able to match not only the risk-neutral dynamics but also the physical dynamics and risk premia individually.

5.2 Out-of-sample fit

We now turn to a much more stringent test of model performance: the analysis of goodness-of-fit for equity and credit index derivative markets out-of-sample.

5.2.1 SPX options

Most approaches in the option literature consist of fitting reduced-form option pricing models directly to the data, on which they are subsequently evaluated. In contrast, our model is estimated using the term structure of CDX spreads and physical SPX volatility, without any

price information from options. It is thus natural to ask how well the model performs in pricing SPX options. The out-of-sample nature of this exercise contrasts with the standard approach, and a strong performance here could be seen as a contribution in itself.

We calculate the prices of SPX options using our estimated model with the filtered state variables displayed in Figure 2. For comparison with the data, the model prices are converted into Black-Scholes-implied volatilities. Panel A of Figure 4 plots the time series of at-the-money implied volatilities in the data (yellow solid line) and in the model (blue dotted line). It is clear that the model-implied volatilities match the overall magnitude of the data-implied volatilities well. Paying closer attention, we see that the model-implied volatilities also closely track empirical time series fluctuations. The timings of the spikes in implied volatilities predicted by the model during the Global Financial Crisis, the European sovereign debt crisis, and the COVID-19 crisis coincide almost perfectly with the data. There are a few observations where the magnitudes of the model and data estimates diverge. Yet, the results suggest that our model is able to address not only the level but also the overall time series variation of SPX option prices.

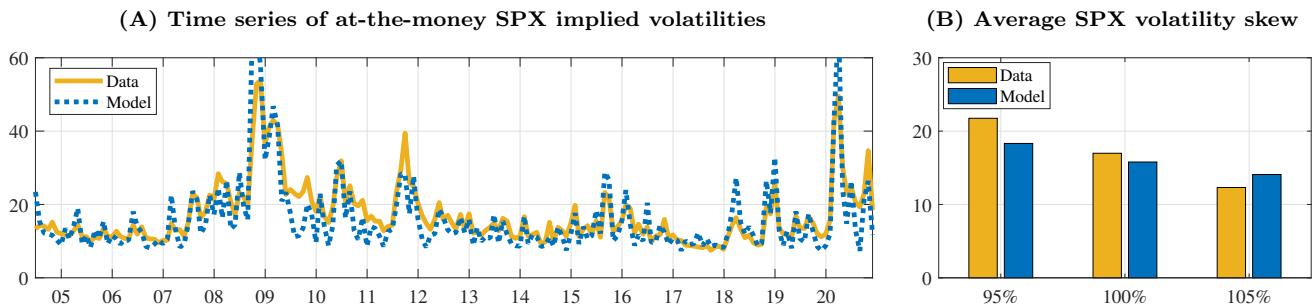


Figure 4: SPX implied volatilities. The figure compares the Black-Scholes-implied volatilities for SPX options in the data and in the model. Panel A plots the time series of at-the-money SPX implied volatilities in the data (yellow solid line) and in the model (blue dotted line). Panel B presents the average SPX implied volatilities with moneyness of 95, 100, and 105% in the data (yellow bars) and in the model (blue bars). The implied volatilities are expressed in percentages. The data frequency is monthly, where the data and model values are sampled at the end of each month. The implied volatilities are expressed in percentages. The sample period is from June 2004 to November 2020.

Next, we check if our model can explain the cross-section of SPX implied volatilities across different moneyness values, which is commonly referred to as the implied volatility skew. In Panel B of Figure 4, we juxtapose the average implied volatilities for SPX options with

moneyiness of 95, 100, and 105% in the data (yellow bars) and in the model (blue bars). Granted, the model fit is not perfect, which is to be expected given the out-of-sample nature of the exercise; the predicted slope is slightly less steep than what is observed empirically. However, the model generates a negative volatility skew that is close to the data. The economic magnitude of the discrepancy between the data and the model is relatively small on average.

To quantify model performance, Table 5 reports the means and standard deviations of SPX implied volatilities in the data (Panel A) and in the model (Panel B). The magnitude of the pricing errors varies across moneyiness. The model tends to underprice out-of-the-money puts (moneyiness of 95%), contracts that are notoriously hard to explain. In contrast, the model overprices in-the-money puts (moneyiness of 105%) on average. Yet, the model fits at-the-money options well. The standard deviations of the model-implied volatilities are also fairly close to those found in the data. This observation is reinforced by the high correlations between the data and the model and the small magnitudes of the RMSEs reported in Panel C.

K/I_t	(A) Data		(B) Model		(C) Fit	
	Mean	Std.	Mean	Std.	Corr.	RMSE
95%	21.75	8.04	18.32	9.56	0.88	5.64
100%	16.98	8.32	15.79	9.99	0.89	4.82
105%	12.31	8.70	14.08	10.03	0.88	5.11

Table 5: Out-of-sample model fit for SPX options. The table examines the out-of-sample fit for SPX options. Panels A and B report the sample means and standard deviations of Black-Scholes-implied volatilities for SPX options with moneyiness of 95, 100, and 105% in the data and in the model. In Panel C, we present two goodness of fit metrics to assess model performance: the time-series correlation between the data and the model as well as the root mean squared error (RMSE). The measurement frequency is monthly, where the data and model values are sampled at the end of each month. The sample period is from June 2004 to November 2020.

5.2.2 CDX options

Our second out-of-sample exercise is to test whether the estimated model can predict the prices of CDX options. This is of particular interest, given that the model captures the price patterns of SPX options well. So far, the main result documented by Collin-Dufresne, Junge, and Trolle (2022) suggests that the pricing of CDX and SPX options are hard to reconcile,

potentially due to a lack of market integration. However, the exercise in Section 4.3 shows that our model can generate reasonable CDX implied volatilities when the two state variables are freely chosen to fit the CDX spread and SPX implied volatility, in the spirit of Collin-Dufresne, Junge, and Trolle (2022)’s empirical design. This only provides a partial resolution to the relative pricing puzzle. In our setup, the state variables are stochastic processes with their own dynamics. Thus, analyzing the model performance in the time series using the filtered state variables as input could lead to a different conclusion than what we found in the static case.

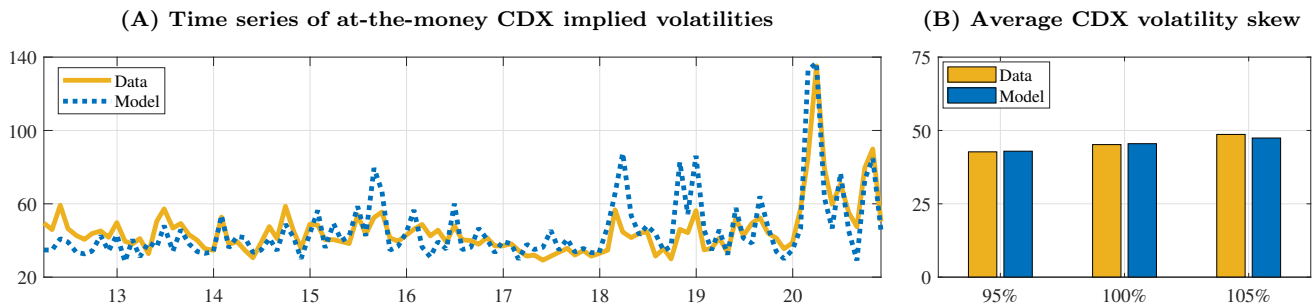


Figure 5: CDX implied volatilities. The figure compares the Black-implied volatilities for CDX options in the data and in the model. Panel A plots the time series of at-the-money CDX implied volatilities in the data (yellow solid line) and in the model (blue dotted line). Panel B presents the average CDX implied volatilities with moneyness of 95, 100, and 105% in the data (yellow bars) and in the model (blue bars). The implied volatilities are expressed in percentages. The data frequency is monthly, where the data and model values are sampled at the end of each month. The implied volatilities are expressed in percentages. The sample period is from March 2012 to November 2020.

To visualize the model’s prediction over time, Panel A of Figure 5 plots the time series of at-the-money Black-implied volatilities for CDX options in the data (yellow solid lines) and in the model (blue dotted lines). As discussed in Section 3.1, these option contracts are relatively new financial instruments that began trading with significant volumes in 2012. Accordingly, the sample for this exercise is shorter, spanning the period from March 2012 to November 2020. While the model tracks the time series patterns in the data fairly well, we do see a few more outliers than for the SPX. These correspond to episodes with sharp volatility spikes in the equity market. Our model correctly translates these spikes into abrupt increases in CDX implied volatilities but somewhat exaggerates their magnitude. Apart from these outliers, the model fit is generally good.

Most importantly, Panel A suggests that the model successfully captures the level of CDX implied volatilities in the data and that no pervasive mispricing is apparent. This is also clear from Panel B of Figure 5 where we plot the average implied volatilities for CDX options with moneyness of 95, 100, and 105%. The model produces a positive volatility skew that lines up almost perfectly with the data.

Table 6 investigates the pricing performance of our model in further detail. Comparing Panels A and B, we can see that the errors in implied volatilities are small in magnitude across the board, less than 1% in absolute value. The standard deviations of the model-implied volatilities are larger in magnitude than their empirical counterparts, as the model time series occasionally exaggerates extreme movements relative to the data (Panel A of Figure 5). Panel C examines the quality of model fit. The time series fit for CDX options is comparable to that for SPX options but delivers slightly lower correlations with the data. Still, considering that the predictions are out-of-sample, the correlations between the data and the model for CDX options are high (0.77-0.80) and the RMSEs are moderate (around 11%). As a point of reference, the pricing errors for CDX options reported in Collin-Dufresne, Junge, and Trolle (2022) when fitting their model to CDX options are about 30% in relative terms.²¹

K/I_t	(A) Data		(B) Model		(C) Fit	
	Mean	Std.	Mean	Std.	Corr.	RMSE
95%	42.71	14.18	42.93	19.12	0.77	12.12
100%	45.18	14.24	45.49	18.20	0.79	11.17
105%	48.65	13.97	47.42	17.55	0.80	10.65

Table 6: Out-of-sample model fit for CDX options. The table examines the out-of-sample fit for CDX options. Panels A and B report the sample means and standard deviations of Black-implied volatilities for CDX options with moneyness of 95, 100, and 105% in the data and in the model. In Panel C, we present two goodness of fit metrics to assess model performance: the time-series correlation between the data and the model as well as the root mean squared error (RMSE). The measurement frequency is monthly, where the data and model values are sampled at the end of each month. The sample period is from March 2012 to November 2020.

Overall, the model CDX implied volatilities match their empirical counterparts well unconditionally and in the time series. We do not observe clear disparities nor mispricing, contrary

²¹See Table 5 in Collin-Dufresne, Junge, and Trolle (2022).

to the findings of Collin-Dufresne, Junge, and Trolle (2022).

5.3 Implications for option returns and risk premia

Having validated our model’s performance for the pricing of the CDX and SPX/CDX options, we can now turn to its implications for option returns and risk premia. Previous studies have examined the returns on SPX options, yet the question of whether their levels are reasonable or suggest instances of mispricing remains a topic of debate. Moreover, there is very little work on CDX options, let alone their returns. In addition to studying option returns in two markets jointly and out-of-sample, to the best of our knowledge, we are the first to do so with a structural model.

In Table 7, we compare the average excess returns calculated from the data with the expected excess returns implied by the model. We again consider 1-month SPX and CDX calls and puts with moneyness of 95, 100, and 105%. For the data, we calculate the annualized sample mean of daily excess returns on each option. For the model, we obtain the instantaneous expected excess return by evaluating equation (14) at the average filtered state variables. Reported together are the p -values of the null hypothesis that the model is correct. We compute them by simulating the model-implied finite-sample distribution of the average excess return in a similar spirit to Broadie, Chernov, and Johannes (2009). If the average excess returns from the data are unlikely to be obtained from the model simulation, the p -values are determined to be small and the model is rejected.

Panel A presents the results for SPX options. As previously documented, average option returns are very large in absolute value. Bondarenko (2014) finds in a sample over 1987-2000 that 1-month at-the-money puts have an annual return of -468%. In an overlapping sample from 1987 to 2005, Broadie, Chernov, and Johannes (2009) calculate the average 1-month ATM put return to be -360%. During our sample period, the average return is -292%, whereas our model predicts it to be -214%. The return on the corresponding call contracts is on average 163% compared to the predicted value of 138%. The panel also shows that the average and predicted returns vary systematically across contracts and moneyness.

	(A) SPX options			(B) CDX options		
	Data	Model	p -value	Data	Model	p -value
Call 95% (ITM)	94.58	89.73	0.29	-310.54	-231.55	0.11
Call 100% (ATM)	163.62	138.07	0.80	-440.08	-274.33	0.27
Call 105% (OTM)	139.13	277.31	0.94	-586.35	-324.30	0.56
Put 95% (OTM)	-555.10	-471.47	0.56	389.85	213.43	0.22
Put 100% (ATM)	-292.37	-214.28	0.47	222.56	181.19	0.74
Put 105% (ITM)	-112.69	-115.70	0.97	178.53	157.36	0.85

Table 7: Average excess returns vs. expected excess returns. The table compares the average excess returns calculated from the data and the expected excess returns implied by the model. Panel A presents the results for SPX options, whereas Panel B presents the results for CDX options. In both cases, we consider 1-month calls and puts with moneyness of 95, 100, and 105%. For the data, we calculate the annualized sample mean of daily excess returns on each option. For the model, we obtain the instantaneous expected excess return by evaluating equation (14) at the average filtered state variables. The p -value for each option is calculated by simulating the model-implied finite-sample distribution of the average excess return. All returns are annualized and expressed in percentages. The sample period is from June 2004 to November 2020 for SPX options (Panel A) and from March 2012 to November 2020 for CDX options (Panel B).

Calls experience positive returns while average put returns are negative. Out-of-the-money contracts for both calls and puts have higher returns in absolute value than in-the-money contracts. For example, the average return on out-of-the-money calls is almost twice that of in-the-money calls. The model captures these qualitative patterns fairly well, although the quantitative fit does not seem to be perfect.

It is important to bear in mind that the empirical estimates in Table 7 correspond to the average returns from one particular realized path of the economy. To discuss the model fit, we need to take into account the sampling distribution of the average excess return. Since options returns are extreme with high skewness and kurtosis, the apparent gap between the data and the model may not be statistically significant. The p -values reported in Panel A confirm this intuition. All of the p -values well exceed 0.1, implying that we cannot statistically distinguish the data estimates from the model predictions for any option class, not just at the 5% but also at the 10% significance level. Put differently, it is not too unlikely to observe average excess returns that are similar to the empirical ones when we simulate the model.

Hence, we find no evidence of a systematic bias in terms of SPX option returns. This echoes Broadie, Chernov, and Johannes (2009) but in the context of a structural model that accounts for risk premia for both stochastic volatility and systematic jumps. They test whether the

data deviate from simulated option returns in the model of Black and Scholes (1973) or Heston (1993) and find no significant evidence of mispricing. More recently, however, Chambers, Foy, Liebner, and Lu (2014) revisit their study with a longer sample and document more mixed results. Our analysis with SPX options can be seen as supporting and corroborating the results from Broadie, Chernov, and Johannes (2009): allowing for priced variance risk and jump risk, we find no support for systematic mispricing.

Now we turn to the results for CDX options in Panel B. As discussed in Section 4.2, CDX calls and SPX puts are downmarket instruments, whereas CDX puts and SPX calls pay out in good economic states. In line with this intuition, we can see that the average excess returns on CDX calls, like on SPX puts, are negative whereas those on CDX puts and SPX calls are positive. Empirically, we find that out-of-the-money CDX calls have higher average excess returns (in absolute value) than out-of-the-money CDX puts. Our model captures these relative patterns across option classes and markets well.

The p -values reported in Panel B indicate, again, that we cannot reject the model quantitatively. The average excess returns on out-of-the-money calls and puts are -586% and 390% in the data, which is quite a bit higher than the model predictions of -324% and 213%, respectively. Nevertheless, the data values are not statistically different from the model estimates, considering the sampling distribution. Overall, this points to a conclusion similar to the case for SPX options: there is no strong evidence of CDX option mispricing.

Table 8 now decomposes model expected excess returns into risk premia associated with the three sources of systematic risk. We observe that the signs of individual risk premia are consistent with our intuition. First, consider the asset risk premium. On the one hand, SPX calls and CDX puts are instruments that pay out more in good economic times with higher asset values and pay out less in bad economic times with lower asset values ($\Delta_{A,t} > 0$ in Figure 1). In other words, these instruments make good times better but bad times worse. All else equal, investors dislike such instruments, demanding a positive risk premium as extra compensation. On the other hand, SPX puts and CDX calls pay out more when asset values fall and pay out less when asset values rise (i.e., $\Delta_{A,t} < 0$ in Figure 1). Since they serve as a

hedge, investors are eager to hold them, inducing a negative asset risk premium.

(A) SPX options							
	Total	=	Asset risk	+	Variance risk	+	Jump risk
Call 95% (ITM)	89.73 [100%]		97.59 [109%]		-15.53 [-17%]		7.67 [9%]
Call 100% (ATM)	138.07 [100%]		164.91 [119%]		-38.97 [-28%]		12.13 [9%]
Call 105% (OTM)	277.31 [100%]		328.23 [118%]		-73.73 [-27%]		22.81 [8%]
Put 95% (OTM)	-471.47 [100%]		-336.74 [71%]		-93.86 [20%]		-40.87 [9%]
Put 100% (ATM)	-214.28 [100%]		-156.99 [73%]		-39.13 [18%]		-18.17 [8%]
Put 105% (ITM)	-115.70 [100%]		-92.54 [80%]		-13.02 [11%]		-10.14 [9%]
(B) CDX options							
	Total	=	Asset risk	+	Variance risk	+	Jump risk
Call 95% (ITM)	-231.55 [100%]		-107.05 [46%]		-112.21 [48%]		-12.28 [5%]
Call 100% (ATM)	-274.33 [100%]		-127.81 [47%]		-131.53 [48%]		-14.99 [5%]
Call 105% (OTM)	-324.30 [100%]		-153.60 [47%]		-152.29 [47%]		-18.40 [6%]
Put 95% (OTM)	213.43 [100%]		149.71 [70%]		52.46 [25%]		11.26 [5%]
Put 100% (ATM)	181.19 [100%]		118.34 [65%]		53.71 [30%]		9.15 [5%]
Put 105% (ITM)	157.36 [100%]		96.81 [62%]		52.85 [34%]		7.70 [5%]

Table 8: Risk premium decomposition. The table decomposes the expected excess returns from the model into three risk premia: asset risk premium, variance risk premium, and jump risk premium. Panel A presents the results for the SPX and SPX options, whereas Panel B presents the results for the CDX and CDX options. Reported together in square brackets are percentage shares of individual risk premia to the total risk premium. The decomposition is obtained by evaluating equation (14) at the average filtered state variables. All returns are annual and expressed in percentages.

Similarly, the sign of the variance risk premium depends on the sign of the variance risk exposure $\Delta_{V,t}$ in Figure 1. Instruments that are positively exposed to variance risk, such as SPX calls and puts as well as CDX calls, provide a hedge against variance risk, as they pay out more in bad times with high asset variance. Hence, investors are willing to accept a negative variance risk premium for holding these instruments. In contrast, for CDX puts, the variance risk premium is positive as they are negatively exposed to variance risk.

Note that the jump risk premium has the same sign as the asset risk premium for all options. This is not a coincidence. Jumps directly impact the level of assets. For instance, large negative jumps result in lower asset value. Thus, instruments whose prices decrease in tandem with a firm's assets will command a positive jump premium. Therefore, the signs of the jump risk premium $\lambda_t^m \mathbb{E}_{Z^m}[-\Delta_{N,t}(e^{\xi_m Z_t^m} - 1)]$ and the asset risk premium $\Delta_{A,t}(\mu_t - r_f)$ in equation (14) are the same.

In terms of magnitudes, Table 8 shows that the relative importance of each risk premium

component varies depending on the option. We report the percentage contribution of individual risk premia to the total risk premium in square brackets. For SPX options, the asset risk premium accounts for the lion's share of total risk premia. This component even exceeds 100% of the total risk premium for SPX calls, as the variance risk premium is negative.

For CDX options, the ordering of systematic risk contributions depends on the option payoff. For calls, the asset risk premium is at par with the variance risk premium. For puts, the asset risk premium is about twice as large as the variance risk premium. Most interestingly, we find that for CDX calls the variance risk premium is much more predominant than the asset risk premium relative to SPX puts. This is because the CDX is more sensitive to variance risk than the SPX, as discussed in Section 4.2.

In summary, our model predicts returns that are broadly consistent with what we observe empirically for both SPX and CDX options. It also provides valuable insights into the relative importance of the three sources of risk in determining expected option returns.

6 Conclusion

In this paper, we build an internally consistent model for the valuation of corporate securities, market indices, and index options. We find that our model can address the level and time variation of the implied volatilities for equity and credit index options well out-of-sample. Our results are relevant in light of recent work suggesting that prices of equity and credit index options are hard to reconcile. Our analysis indicates that credit index options are not significantly overpriced nor systematically misaligned with equity index options. Within our model framework, both option markets are very much consistent in terms of their pricing.

After validating our model's ability to match empirical option prices, we examine its implications for option returns. The model does well in explaining average returns on both equity and credit index options, and a rigorous statistical analysis fails to reject its predictions. Although average options returns are strikingly high in absolute value, our model suggests these average returns are fair compensation for the relevant sources of risk.

The structural nature of our model enables us to capture three key sources of systematic

risk, which play a critical role in establishing pricing consistency across the two markets. For each instrument, we analyze risk exposures and discuss the way they impact price dynamics. We provide insights on how the expected return on credit and equity derivative products can be decomposed into asset, variance, and jump risk premia. We show that heterogeneity in exposures to the three sources of risk drives the cross-sectional variation in prices and expected returns observed across the two option markets.

Overall, our analysis demonstrates that a structural compound option framework like ours offers a promising avenue for deepening our understanding of derivative markets and the relevant sources of risk driving their dynamics and return compensations.

Appendix

A CDS pricing and returns

Consider a CDS contract that is written on firm j . The risky PV01 is defined as the present value of future premium payments when the running spread paid by the protection seller is 1 bp per annum. This is computed in our model as

$$\text{RPV01}(A_t^j, V_t, T) = 0.0001 \times \sum_{i=1}^{4T} e^{-r_f(t_i-t)} [1 - G(A_t^j, V_t, t_i)] / 4,$$

where T is the maturity of the given CDS contract and $\{t_1, t_2, \dots, t_{4T}\}$ denote quarterly premium payment dates. As defined earlier, $G(A_t^j, V_t, t_i) = \mathbb{E}_t^{\mathbb{Q}} [\mathbf{1}_{\tau_j \leq t_i}]$ represents the cumulative risk-neutral default probability.

Similarly, the protection leg is defined as the present value of a contingent protection payment. We calculate this in our model as follows:

$$\text{ProtLeg}(A_t^j, V_t, T) = (1 - R) \sum_{i=1}^{4T} e^{-r_f(t_i-t)} [G(A_t^j, V_t, t_i) - G(A_t^j, V_t, t_{i-1})].$$

Here, R represents the recovery rate, measured as a fraction of the CDS notional value.

While the fair market spread (or CDS spread) is determined by $S_t^j = \text{ProtLeg}_t^j / \text{RPV01}_t^j$,

as in equation (10), in practice, a standard CDS contract is traded with a fixed coupon of 100 bp. Instead, the protection buyer and seller exchange an upfront fee U_t^j at the beginning of the contract. This fee is a required side payment to compensate the difference between the fair market spread and the standardized coupon: $U_t^j + 100 \times \text{RPV01}_t^j = \text{ProtLeg}_t^j$. Therefore, the upfront fee is obtained in our model using the following equation:

$$U(A_t^j, V_t, T) = \text{ProtLeg}(A_t^j, V_t, T) - 100 \times \text{RPV01}(A_t^j, V_t, T). \quad (\text{A.1})$$

While the CDS spread and the upfront fee are two different trading/quoting conventions, they are in fact equivalent. Combining equations (A.1) and (10) results in a simple relation: $U_t^j = [S_t^j - 100] \times \text{RPV01}_t^j$. The distinction between the two is merely a matter of convention.

We define the return on a CDS contract by hypothesizing a fully collateralized contract with a dollar notional value. When entering into this contract at time t , the protection seller earns the upfront fee U_t^j . Thus, the protection seller needs to make a payment of $1 - U_t^j$ at inception to put a dollar collateral. Assuming that the dollar collateral earns the risk-free rate r_f , the payoff of the contract at time $t + \Delta t$ consists of the following three components: (i) receiving the original collateral back with interest (i.e., $1 + r_f \Delta t$), (ii) collecting the standardized CDS premium, which is fixed at 100 bp (i.e., $0.01 \Delta t$), and (iii) paying the cost of unwinding the protection sell position at time $t + \Delta t$ (i.e., $-U_{t+\Delta t}^j$). This implies that from the protection seller's point of view, the excess return on the CDS contract can be calculated by

$$\frac{1 + r_f \Delta t + 0.01 \Delta t - U_{t+\Delta t}^j}{1 - U_t^j} - r_f \Delta t = \underbrace{\frac{P_{t+\Delta t}^j - P_t^j}{P_t^j}}_{\text{Capital gains}} + \underbrace{\frac{0.01}{P_t^j} \Delta t}_{\text{Premium yield}} + \underbrace{r_f \left(\frac{1}{P_t^j} - 1 \right) \Delta t}_{\text{Net opportunity cost}},$$

where $P_t^j = 1 - U_t^j$ and $P_{t+\Delta t}^j = 1 - U_{t+\Delta t}^j$ are often referred to as the CDS prices. By taking the limit of $\Delta t \rightarrow 0$, the expression for the instantaneous excess return, which is useful for our continuous-time setup, is given by

$$\frac{dP_t^j}{P_t^j} + \left[\frac{0.01}{P_t^j} + r_f \left(\frac{1}{P_t^j} - 1 \right) \right] dt.$$

References

- Aït-Sahalia, Yacine, and Robert L Kimmel, 2010, Estimating affine multifactor term structure models using closed-form likelihood expansions, *Journal of Financial Economics* 98, 113–144.
- Andersen, Torben G, Nicola Fusari, and Viktor Todorov, 2020, The pricing of tail risk and the equity premium: Evidence from international option markets, *Journal of Business & Economic Statistics* 38, 662–678.
- Andersen, Torben G, Viktor Todorov, and Masato Ubukata, 2021, Tail risk and return predictability for the Japanese equity market, *Journal of Econometrics* 222, 344–363.
- Bakshi, Gurdip, Charles Cao, and Zhiwu Chen, 1997, Empirical Performance of Alternative Option Pricing Models, *The Journal of Finance* 52, 2003–2049.
- Bates, David S., 2000, Post-'87 crash fears in the S&P 500 futures option market, *Journal of Econometrics* 94, 181–238.
- Bates, David S, 2003, Empirical option pricing: A retrospection, *Journal of Econometrics* 116, 387–404.
- Berger, David, Ian Dew-Becker, and Stefano Giglio, 2020, Uncertainty shocks as second-moment news shocks, *Review of Economic Studies* 87, 40–76.
- Black, Fischer, 1976, Studies of stock price volatility changes, *Proceedings of the 1976 Meetings of the American Statistical Association, Business and Economic Statistics Section* pp. 177–181.
- Black, Fischer, and John C Cox, 1976, Valuing corporate securities: Some effects of bond indenture provisions, *The Journal of Finance* 31, 351–367.
- Black, Fischer, and Myron Scholes, 1973, The Pricing of Options and Corporate Liabilities, *Journal of Political Economy* 81, 637–654.
- Bondarenko, Oleg, 2014, Why are put options so expensive?, *Quarterly Journal of Finance* 4, 1–50.
- Broadie, Mark, Mikhail Chernov, and Michael Johannes, 2009, Understanding Index Option Returns, *The Review of Financial Studies* 22, 4493–4529.
- Cao, Jie, Amit Goyal, Xiao Xiao, and Xintong Zhan, 2022, Implied Volatility Changes and Corporate Bond Returns, *Management Science* pp. 1–23.
- Carr, Peter, and Liuren Wu, 2009, Variance risk premiums, *Review of Financial Studies* 22, 1311–1341.
- Carr, Peter, and Liuren Wu, 2011, A simple robust link between American puts and credit protection, *Review of Financial Studies* 24, 473–505.
- Chambers, Donald R., Matthew Foy, Jeffrey Liebner, and Qin Lu, 2014, Index Option Returns: Still Puzzling, *Review of Financial Studies* 27, 1915–1928.
- Chen, Long, Pierre Collin-Dufresne, and Robert S Goldstein, 2009, On the relation between the credit spread puzzle and the equity premium puzzle, *The Review of Financial Studies*

22, 3367–3409.

- Chen, Steven Shu-Hsiu, Hitesh Doshi, and Sang Byung Seo, 2023, Synthetic Options and Implied Volatility for the Corporate Bond Market, *Journal of Financial and Quantitative Analysis* 58, 1295–1325.
- Choi, Yong Seok, Hitesh Doshi, Kris Jacobs, and Stuart M. Turnbull, 2019, Pricing structured products with economic covariates, *Journal of Financial Economics*.
- Christoffersen, Peter, Mathieu Fournier, and Kris Jacobs, 2018, The factor structure in equity options, *Review of Financial Studies* 31, 595–637.
- Christoffersen, Peter, Kris Jacobs, Chayawat Ornthanalai, and Yintian Wang, 2008, Option valuation with long-run and short-run volatility components, *Journal of Financial Economics* 90, 272–297.
- Collin-Dufresne, Pierre, Robert S. Goldstein, and Fan Yang, 2012, On the relative pricing of long-maturity index options and collateralized debt obligations, *Journal of Finance* 67, 1983–2014.
- Collin-Dufresne, Pierre, Benjamin Junge, and Anders B Trolle, 2022, How Integrated Are Credit and Equity Markets? Evidence From Index Options, Forthcoming, *Journal of Finance*.
- Coval, Joshua D., and Tyler Shumway, 2001, Expected option returns, *Journal of Finance* 56, 983–1009.
- Cox, John C., Jonathan C. Ingersoll, and Stephen A. Ross, 1985, A theory of the term structure of interest rates, *Econometrica* 53, 385–408.
- Cremers, K. J. Martijn, Joost Driessen, and Pascal Maenhout, 2008, Explaining the level of credit spreads: Option-implied jump risk premia in a firm value model, *Review of Financial Studies* 21, 2209–2242.
- Culp, Christopher L., Yoshio Nozawa, and Pietro Veronesi, 2018, Option-based credit spreads, *American Economic Review* 108, 454–88.
- Davydenko, Sergei, 2012, When do firms default? A study of the default boundary, Working Paper, University of Toronto.
- Du, Du, Redouane Elkamhi, and Jan Ericsson, 2019, Time-Varying Asset Volatility and the Credit Spread Puzzle, *Journal of Finance* 74, 1841–1885.
- Duffee, Gregory R., 2002, Term premia and interest rate forecasts in affine models, *Journal of Finance* 57, 369–443.
- Eraker, Bjørn, 2004, Do stock prices and volatility jump? Reconciling evidence from spot and option prices, *Journal of Finance* 59, 1367–1404.
- Eraker, Bjørn, Michael Johannes, and Nicholas Polson, 2003, The impact of jumps in volatility and returns, *Journal of Finance* 58, 1269–1300.
- Eraker, Bjørn, and Jiakou Wang, 2015, A Non-linear Dynamic Model of the Variance Risk Premium, *Journal of Econometrics* 187, 547–556 Econometric Analysis of Financial Deriva-

tives.

- Feldhütter, Peter, and Stephen M Schaefer, 2018, The myth of the credit spread puzzle, *The Review of Financial Studies* 31, 2897–2942.
- Geske, Robert, 1979, The valuation of compound options, *Journal of Financial Economics* 7, 63–81.
- Heston, Steven L., 1993, A Closed-Form Solution for Options with Stochastic Volatility with Applications to Bond and Currency Options, *Review of Financial Studies* 6, 327–343.
- Jones, Christopher S., 2006, A Nonlinear Factor Analysis of S&P 500 Index Option Returns, *Journal of Finance* 61, 2325–2363.
- Leland, Hayne E, 1994, Corporate debt value, bond covenants, and optimal capital structure, *Journal of Finance* 49, 1213–1252.
- Merton, Robert C., 1974, On the pricing of corporate debt: The risk structure of interest rates, *Journal of Finance* 29, 449–470.
- Pan, Jun, 2002, The jump-risk premia implicit in options: Evidence from an integrated time-series study, *Journal of Financial Economics* 63, 3–50.
- Seo, Sang Byung, and Jessica A. Wachter, 2018, Do rare events explain CDX tranche spreads?, *Journal of Finance* 73, 2343–2383.
- Todorov, Viktor, 2010, Variance risk-premium dynamics: The role of jumps, *Review of Financial Studies* 23, 345–383.
- Vasicek, Oldrich, 2002, The distribution of loan portfolio value, *Risk* 15, 160–162.